9B

PNL-5013
UC-25

Sputter-Deposited Metallic and Ceramic Coatings for Heat Engines

Work Performed from October 1980
to September 1983

J. T. Prater
R. W. Moss

April 1984

Prepared for the U.S. Department of Energy
under Contract DE-AC06-76RLO 1830

Pacific Northwest Laboratory
Operated for the U.S. Department of Energy
by Battelle Memorial Institute

Battelle

PNL-5013

DISCLAIMER

PACIFIC NORTHWEST LABORATORY
operated by
BATTELLE
for the
UNITED STATES DEPARTMENT OF ENERGY
under Contract DE-AC06-76RLO 1830

Printed in the United States of America
Available from
National Technical Information Service
United States Department of Commerce
5285 Port Royal Road
Springfield, Virginia 22161

NTIS Price Codes
Microfiche A01

Printed Copy

Pages	Price Codes
001-025	A02
026-050	A03
051-075	A04
076-100	A05
101-125	A06
126-150	A07
151-175	A08
176-200	A09
201-225	A010
226-250	A011
251-275	A012
276-300	A013

PNL-5013
UC-25

SPUTTER-DEPOSITED METALLIC AND CERAMIC COATINGS FOR HEAT ENGINES

Work Performed from October 1980
to September 1983

J. T. Prater
R. W. Moss

April 1984

Prepared for
the U.S. Department of Energy
under Contract DE-AC06-76RLO 1830

Pacific Northwest Laboratory
Richland, Washington 99352

ACKNOWLEDGMENTS

The authors wish to thank H. E. Kjarmo, for providing x-ray diffraction and scanning microscopy; R. H. Beauchamp, for preparing optical metallography; J. W. Johnston and R. F. Stratton, for preparing the sputtered coatings; and A. G. Graybeal, for preparing the plasma-sprayed coatings. L. F. Aprigliano at the David W. Taylor Naval Ship Research and Development Center and J. R. Nicholls and P. Hancock at the Cranfield Institute of Technology provided the burner rig test facilities and the depth of attack measurements on the metallic coatings. J. W. Patten provided technical advice and guidance during the course of the research program; and S. K. Edler provided editorial assistance.

ABSTRACT

Progress in the development of metallic and ceramic coatings with improved high-temperature corrosion and erosion/wear resistance is reported. The objective was to develop coatings that would insure that future heat engines, notably gas turbines and diesels, would be able to operate efficiently on degraded fuel supplies. The majority of coatings investigated were prepared by sputter deposition. Research on sputter-deposited CoCrAlY coatings was directed at improving their low-temperature, hot corrosion resistance by introducing composition gradients and adding platinum. Studies on sputter-deposited ZrO_2 and Al_2O_3 coatings were conducted to improve the thermal cycling resistance of ceramic deposits on metal substrates by using combinations of graded transition layers, columnar ceramic structures, and dense sealing layers. Preliminary results on plasma-sprayed Ni-SiC and quartz-SiC coatings that showed good wear and oxidation resistance are also reported.

EXECUTIVE SUMMARY

Metallic and ceramic coatings have been investigated to identify coatings that can provide improved erosion, corrosion, and wear resistance to insure that future heat engines will be able to operate efficiently on degraded fuel supplies. Current state-of-the-art CoCrAlY coatings were modified to identify compositional changes that would improve the hot corrosion resistance of these coatings and thereby provide near-term solutions. Ceramic coatings were investigated as a potential long-term solution. If the major technical problems associated with the development of these coatings can be overcome, then a new generation of coatings with much better erosion and corrosion resistance will be available. Composite coatings that embedded SiC particles in ductile metal or glass matrices were investigated as prospective wear-resistant coatings.

The corrosion resistance of a series of modified CoCrAlY coatings to different combustion environments was investigated. These burner rig tests simulated atmospheres that would be encountered in the use of alternative fuels. Coating performance depended on the combination of coating composition and combustion environment. Using chromium and aluminum composition gradients through the thickness of the coating and alloying CoCrAlY coatings with platinum were identified as useful coating modifications, although the exact modifications must be correlated with the application. Using platinum underlayers as a diffusion barrier to limit substrate/coating interdiffusion was found to be ineffective.

In an aggressive, low-temperature, hot corrosion environment (simulated by burning doped marine diesel in a burner rig), the coatings with 1) a high chromium surface concentration, 2) a high chromium-to-aluminum ratio at the surface, and 3) an aluminum composition gradient that increased the aluminum concentration into the coating thickness were more corrosion resistant. Deposits of CoCrAlY containing large additions of platinum also provided good low-temperature protection.

A burner rig test with solvent refined coal (SRC-II) provided materials data in an extremely aggressive environment (characteristic of vanadate attack). Of the coatings tested, those with 1) a low chromium surface

concentration, 2) a high aluminum-to-chromium ratio at the surface, and 3) a chromium composition gradient that increased the chromium concentration into the coating thickness were more corrosion resistant.

Experiments were performed to evaluate techniques for improving the adherence of ceramic deposits to metallic substrates. If adherent coatings could be developed, a new generation of corrosion- and erosion-resistant coatings would be available that would offer much greater protection in corrosive environments than currently available metallic coatings. Ceramic coatings with graded metal-to-ceramic transition zones and columnar ceramic structures were assessed.

The following ceramic materials were investigated: $ZrO_2 \cdot 20Y_2O_3$, $ZrO_2 \cdot 8Y_2O_3$, Al_2O_3, and $Al_2O_3 \cdot 40Cr_2O_3$. The majority of the zirconia coatings failed as a result of massive diffusion of aluminum (from the MCrAlY) and oxygen (from the ZrO_2) in the graded metal-to-ceramic layer. Coating fracture occurred very low in the graded transition zone, where a band of Al_2O_3 and voids formed that acted as a preferred path for crack propagation. For this reason, the ZrO_2 coating with no graded transition zone performed the best in thermal cycling experiments. Graded Al_2O_3-CoCrAlY layers were not affected by interdiffusion; however, ceramic layers of $Al_2O_3 \cdot 40Cr_2O_3$ or $ZrO_2 \cdot 20Y_2O_3$ deposited over graded Al_2O_3-CoCrAlY layers did not adhere very well. Multilayered metal/ceramic coatings were judged to have only limited potential, perhaps in erosive low-temperature diesel applications.

Depositing sealing (closeout) layers over the porous ceramic structure (for example, the columnar microstructure of physical vapor deposited coatings) was identified as a potential technique for reducing the permeability of the coating to solid and liquid combustion products without affecting coating adherence. This or a similar sealing technique will be essential for the success of ceramic coatings used in alternative fuel environments.

In wear tests on silicon carbide composite coatings, plasma-sprayed coatings that deposited silicon carbide in either a nickel or quartz matrix had good wear and corrosion resistance. These coatings might be appropriate for use in diesels operated on erosive coal slurries.

CONTENTS

ACKNOWLEDGMENTS..... iii

ABSTRACT..... v

EXECUTIVE SUMMARY..... vii

INTRODUCTION..... 1

METALLIC COATING DEVELOPMENT..... 3

EXPERIMENTAL PROCEDURES..... 4

Coating Preparation..... 4

Coating Evaluation..... 7

RESULTS AND DISCUSSION..... 9

Coating Characterization..... 9

Annapolis NSRDC Burner Rig Test..... 10

Cranfield Institute Burner Rig Test with SRC-II..... 19

Rolls Royce Engine Test with Residual Fuel..... 21

SUMMARY..... 24

CERAMIC COATING DEVELOPMENT..... 27

EXPERIMENTAL PRDCEDURES..... 29

Graded Coatings..... 30

Multilayered Coatings..... 32

RESULTS AND DISCUSSION..... 34

Graded Transition Layers..... 34

Ceramic Closeout Layers..... 44

Multilayered Metal/Ceramic Coatings..... 46

SUMMARY..... 49

SiC-METAL COMPOSITE COATING DEVELOPMENT..... 51

EXPERIMENTAL PROCEDURES AND RESULTS..... 52
Coating Preparation..... 52
Wear Test..... 53
Oxidation Test..... 56
SUMMARY..... 57
CONCLUSIONS..... 59
REFERENCES..... 61

FIGURES

1 Sputtering Chamber Used for Preparation of Metallic Coatings..... 5

2 Sputtering Chamber Used for Deposition of Platinum Underlayers..... 6

3 CoCrAlY Coating Sputter Deposited onto Sputtered Platinum Underlayer..... 11

4 Typical Corrosion Pit on Burner Rig Pins Tested at Annapolis NSRDC..... 12

5 Optical Micrograph Showing a Cross Section of a Graded 27-29% Cr, 6-4% Al Coating..... 15

6 Optical Micrograph Showing a Cross Section of a Graded Pt-CoCrAlY Coating After Burner Rig Test..... 16

7 Optical Micrograph Showing a Cross Section of a Graded 24-30% Cr, 19-3% Al Coating..... 17

8 SEM Micrograph of Platinum Underlayer After 500-h Burner Rig Test..... 18

9 Comparison of Corrosion Attack for a Variety of Sputtered, Graded CoCrAlY, and PVD CoCrAlY Coatings With and Without Platinum Underlayers..... 22

10 Optical Micrograph of CoCrAlY Coating Tested for 42 h in a Rolls Royce Turbine Operated on Residual Fuel..... 23

11 Optical Micrograph of Preoxidized CoCrAlY Coating Tested for 42 h in a Rolls Royce Turbine Operated on Residual Fuel..... 24

12 Sputtering Chamber Used for Preparation of Ceramic Coatings..... 29

13 SEM Micrograph of Fracture Surface Showing Segmented Structure of Sample 2 in the As-Deposited Condition..... 35

14 Optical Micrograph of Sample 3 Following Heat Treatment at 1080°C.... 35

15 Nearly Continuous Alumina Band and Voids Formed in Graded MCrAlY-$ZrO_2 \cdot Y_2O_3$ Layers After Annealing at 1080°C for 8 h..... 38

16 Fracture Surface of Sample 1 Following Three Thermal Cycles to 950°C..... 40

17 Microstructure Produced in Graded MCrAlY-Al_2O_3 Layer of Sample 12 After 8-h Heat Treatment at 1080°C..... 43

18 Examples of Sputtered Closeout Layers Deposited onto Plasma-Sprayed Coatings..... 45

19 Optical Micrograph of Sputtered Nine-Layer Metal/Ceramic Coating..... 47

20 SEM Micrographs of Tensile-Tested Coating Showing Ductile Shear in Ni-50Cr Layers and Fracture Along Columnar Boundaries in the $ZrO_2 \cdot 20Y_2O_3$ Layers..... 48

21 Wear Scar Widths for Different SiC Concentrations and Various Matrix Materials..... 54

TABLES

1 CoCrAlY Coating Variations..... 8

2 Burner Rig Pins Tested at Annapolis NSRDC..... 13

3 Coating Composition Types for Annapolis Burner Rig Test Results..... 14

4 Burner Rig Pins Tested at Cranfield Institute..... 20

5 Coating Composition Types for Cranfield SRC-II Test Results..... 21

6 Rolls Royce Turbine Blade Coating Test Results..... 23

7 Composition of Metal/Ceramic Coatings Tested..... 31

8 Results of Thermal Cycling Experiment..... 36

9 Coefficient of Friction Data for SiC Composite Coatings..... 55

INTRODUCTION

This report describes the results of a research program to provide coatings with improved high-temperature erosion and corrosion resistance. The objective of the program was to develop metallic and ceramic coatings that would insure that future heat engines, notably gas turbines and diesels, would be able to operate efficiently on degraded fuel supplies. The majority of the coatings investigated were prepared by sputter deposition. The work reported in this document was performed between October 1980 and September 1983 by Pacific Northwest Laboratory (PNL)[a] for the U.S. Department of Energy (DOE), Coal Utilization Office, as part of the Combustion Zone Durability (CZD) Program.

The CZD Program is a materials development effort to provide improved coatings for use in future heat engines operated on alternative fuels such as residual oils, shale oils, or coal-derived liquids and gases. The use of these fuels is expected to gradually increase as diminishing supplies and increasing prices reduce the current demand for natural gas and distillate oils. The higher concentration of impurities in these alternative fuels is expected to greatly increase the severity of the corrosive and erosive/wear conditions that combustion zone components will experience. New coatings will be required to adequately protect future engine components in these more severe environments.

PNL research was directed at developing metallic and ceramic coatings for testing in engines operated on alternative fuels. The majority of work utilized PNL-developed sputtering equipment, which offered excellent control over coating composition and structure and permitted detailed studies on the effect these parameters have on coating performance under simulated service conditions.

Metallic coating research was directed at improving the low-temperature, hot corrosion resistance of standard MCrAlY coatings. These coatings were more corrosion resistant when prepared with a composition gradient in aluminum or chromium compared with similar homogeneous coatings. However, to be effective,

(a) Operated for DOE by Battelle Memorial Institute.

the corrosive environment had to be well characterized in advance. Adding platinum to a CoCrAlY coating was also shown to be beneficial in reducing corrosion, while using platinum underlayers proved to be detrimental. The platinum underlayers were ineffective as a diffusion barrier for limiting interdiffusion between the CoCrAlY coatings and the In-792, X-40, or Mar-M-509 substrates.

Ceramic coating research examined techniques for improving the adherence of ceramic deposits to metal substrates. Segmented (columnar) zirconia coatings that were deposited directly onto a CoCrAlY bond layer had the best tolerance to thermal cycling. Multilayered metal/ceramic coatings and ceramic coatings containing either small quantities of retained metal or a thick graded transition layer between the metallic bond layer and the ceramic coating were much less tolerant to thermal cycling. It was also shown that a dense closeout layer could be deposited over a columnar ceramic layer without adversely affecting coating adherence. This closeout layer reduced the permeability of the coating to liquid and gaseous species, which is especially important in extending the lifetime of ceramic coatings that are exposed to the dirtier environments produced by the combustion of many alternative fuels.

Several plasma-sprayed SiC-matrix composite coatings were investigated as potential wear-resistant coatings for use with coal slurry fuels. Preliminary test results are presented. A Ni-SiC and a quartz-SiC coating were found to have good wear and corrosion resistance.

METALLIC COATING DEVELOPMENT

Gas turbine and diesel components operating with current light distillate fuels are often life-limited by hot corrosion effects (oxidation/sulfidation), particularly in marine environments or in the presence of fuel contaminants such as sulfur and vanadium (Stringer 1976). The severity of these effects is expected to increase with the use of residual fuels and increase drastically with the use of minimally processed coal-derived liquid fuels. Because of this concern, a study was initiated to improve existing protective coatings to permit the expanded near-term use of residual and coal-derived liquid fuels in heat engines.

Present state-of-the-art production coatings that were developed to protect gas turbine hot section vanes and blades in hot corrosion environments are variations of MCrAlY (frequently CoCrAlY) compositions. Historically, research has concentrated on coatings prepared by electron beam physical vapor deposition (EB-PVD) techniques (Goward 1978) (Shen, Lee, and Boone 1978) (Grossklaus, Ulion, and Beale 1977). More recently, coatings with these same compositions have been applied by high-rate sputter deposition at PNL. These sputtered coatings are strongly bonded to their substrates, are defect-free, have very fine grain sizes, and have an extremely uniform composition distribution (Patten et al. 1977) (Patten et al. 1979a). Engine and burner rig tests of early sputter-deposited coatings have shown that their performance is comparable with the most advanced PVD coatings. The present study examines several coating composition modifications that offer greater hot corrosion resistance for use in marine environments and for operation with residual and coal-derived fuels.

Coatings were prepared with a variety of chromium and aluminum contents. The selection of the coating composition is important, especially at operating temperatures below 850°C. The optimum composition is expected to be one that promotes the rapid formation of a chromium oxide scale for early protection and then gradually allows the chromium oxide to be replaced by aluminum oxide for long-term oxidation resistance. To achieve this, several coatings were prepared with an aluminum composition gradient that gradually increased the

aluminum concentration at greater depths into the coating. This design provided for a gradual shift towards increased aluminum content in the coating surface region at longer service times, which should enhance the transition of the scale from chromium oxide to aluminum oxide.

As a possible method for reducing the problems that arise from coating/substrate interdiffusion, many of the coatings were prepared with a platinum underlayer that separated the substrate and the CoCrAlY coating. The formation of platinum compounds (for example, platinum alminides) was expected to restrict the mobility of selected elements. Coatings with graded platinum additions were also prepared to establish the optimum distribution of platinum.

The importance of each of these modifications on improving coating corrosion resistance depends on factors such as service temperature, hot corrosion environment, coating and substrate compositions, and coating microstructure. This study has attempted to characterize at least some of these relationships, emphasizing those that are expected to be the most important for future heat engine development.

EXPERIMENTAL PROCEDURES

The experimental procedures that were used in coating preparation and evaluation are discussed in this section.

Coating Preparation

The CoCrAlY coatings were prepared in the dual-target sputtering system shown in Figure 1. Two planar targets (up to 9 in. in diameter) can be accommodated in the system. Research-grade krypton was used as the sputtering gas, and chamber pressures were maintained at ~3 x 10^{-3} torr. Up to seven substrates could be positioned in the sputtering chamber; each substrate was mounted on an individual shaft about midway between the targets. The substrates were rotated at 24 rpm and biased at -35 V dc, relative to the plasma voltage. This slightly negative bias produced sufficient Kr^+ ion bombardment of the substrate surface to disrupt the growth of the columnar defects (leaders) that commonly form as a result of geometric shadowing (Patten 1979). As a result, uniform, defect-free coatings were deposited on relatively

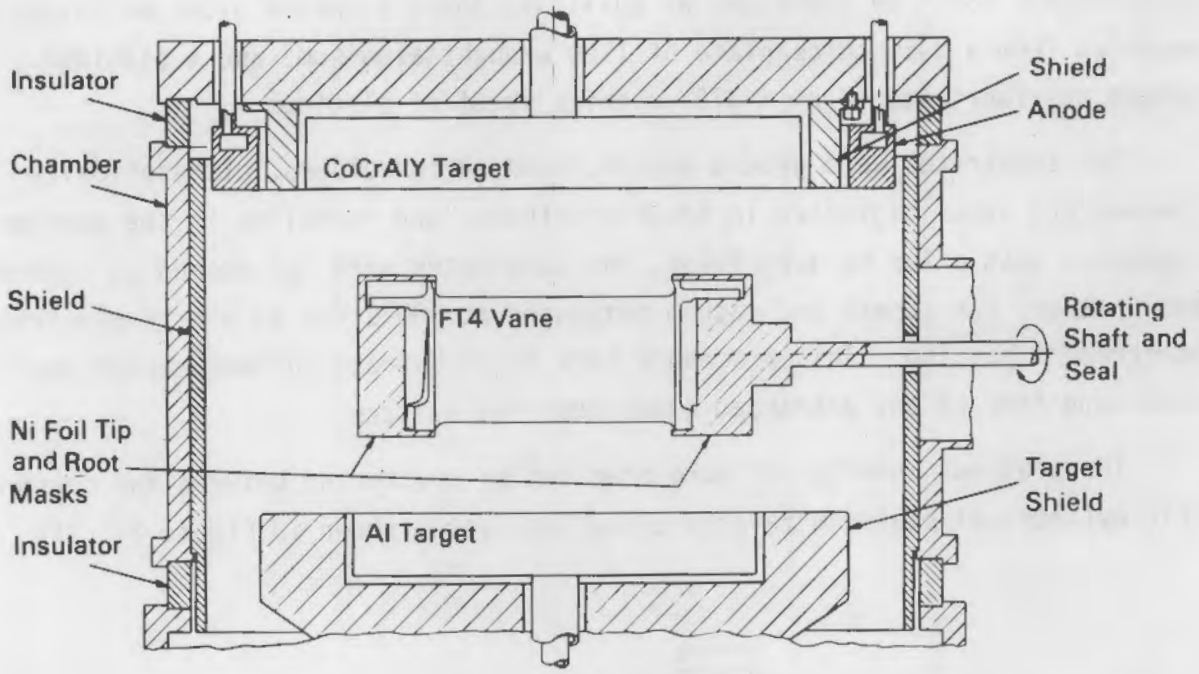

FIGURE 1. Sputtering Chamber Used for Preparation of Metallic Coatings

complex substrate geometries, such as gas turbine blades. No postdeposition processing, such as shot peening, was required to close the defect structure.

Supported plasma dc sputtering was used to obtain high-rate (~20 μm/h) deposition of the metallic layers. By simultaneously sputtering from two independent flat plate targets of CoCrAlY and Al, Cr, or Pt, coatings with different compositions and composition gradients were prepared. The composition of the coating was controlled by regulating the relative power densities applied to the two targets. During a typical deposition experiment, the CoCrAlY target was operated at 20 W/cm^2, and the supplemental metal target was operated at less than 6 W/cm^2 either at a fixed level for homogeneous deposits or in a stepped voltage mode for graded composition deposits.

Three 23-cm diameter CoCrAlY targets were used in the sputtering experiments. All were prepared using hot-pressing techniques developed jointly by PNL and Udimet Powder Division of Special Metals Corp., Ann Arbor, Michigan. The compositions of the three targets were: 1) 22.5 Cr, 14.8 Al, 0.5 Y; 2) 20.6 Cr, 13.5 Al, 0.66 Y; and 3) 30 Cr, 5.8 Al, 1.18 Y. Two 13-cm diameter pure chromium targets were hot-pressed by Haselden, San Jose, California, for

supplemental use. In addition, an auxiliary 23-cm diameter aluminum target was machined from a 2-cm thick plate of 1100 wrought aluminum, and a platinum target was fabricated from a 375-μm thick sheet of platinum.

The substrates were ground smooth, mounted in holders, ultrasonically cleaned and vapor degreased in trichloroethane, and installed in the sputtering chamber. Just prior to deposition, the substrates were ion etched at -100 V and 5 mA/cm^2 for 12 min and vacuum outgassed at 800°C for 15 min by electron bombardment heating. This procedure left the substrate surface exceptionally clean and free of any entrapped gases near the surface.

The platinum underlayers were prepared by sputtering between two concentric cylindrical platinum targets using the system shown in Figure 2. The

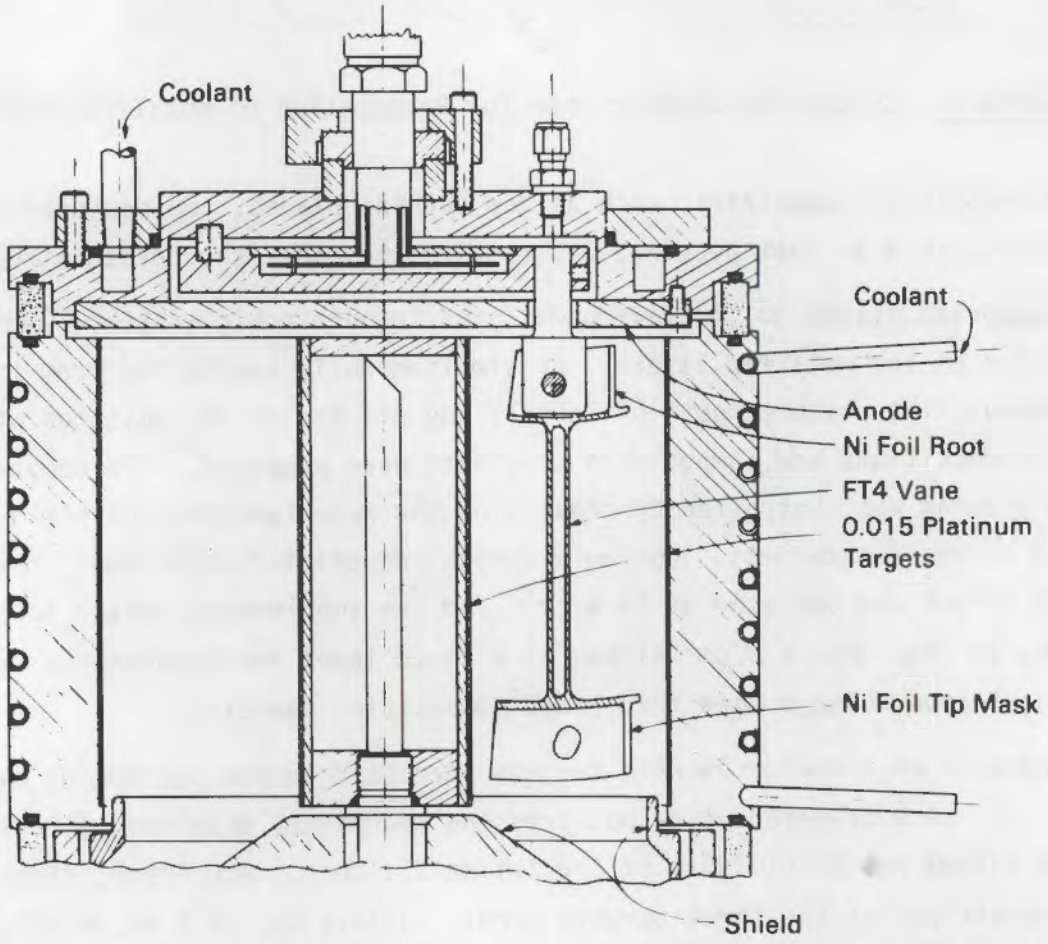

FIGURE 2. Sputtering Chamber Used for Deposition of Platinum Underlayers

targets were formed from 375-μm thick sheets of platinum. This system could accommodate 18 pins or 6 turbine blades at a time. The substrates were not rotated or biased during platinum deposition. The targets were operated at 500 V, with 2.5 and 1.0 amps being drawn on the outer and inner targets, respectively. Under these conditions, a 5-μm platinum layer was deposited in approximately 60 min.

A total of four turbine blades and 210 burner rig test pins were coated for testing and metallographic characterization. The matrix of coating conditions was: 1) eight composition variations, including different chromium and aluminum concentrations and the use of composition gradients through the coating thickness, 2) different heat treatments prior to testing, 3) the presence or absence of platinum underlayers and graded platinum deposits, and 4) deposition on Mar-M-509, X-40, In-792, or In-738 substrates. These coating variations are presented in Table 1. When describing these coatings in the table, composition gradients are denoted by a hyphen; for example, 20-30% Cr signifies that the composition gradient was 20 wt% chromium at the base of the deposit and gradually increased to 30 wt% chromium at the coating surface. An intermediate composition of a coating resulted when the gradient reversed part way through the coating thickness; for example, a 60-90-20% Pt coating had a maximum platinum composition of 90%, which occurred part way through the coating thickness.

Coating Evaluation

Two stages of analysis were performed on the metallic coatings. First, representative coatings were cross sectioned and polished for metallographic examination and characterization in the as-deposited or post-heat-treated condition. The primary analytical technique used for examination was a scanning electron microscope (SEM) equipped with energy dispersive x-ray (EDX) analysis for composition determination. Duplicate pins were then distributed to receptive external facilities for testing in various combustion atmospheres. The intent was to determine those coating parameters that contributed to improved corrosion resistance in as broad a variety of combustion atmospheres as possible.

TABLE 1. CoCrAlY Coating Variations

Coating Compositions	
Homogeneous deposits:	34% Cr, 3% Al 28% ±5% Cr, 9% Al
Graded deposits:[a]	27-29% Cr, 6-4% Al 12-3-21% Cr, 2% Al, 68-87-17% Pt 43-48% Cr, 8-7% Al 24-30% Cr, 19-3% Al 25-30% Cr, 9-8% Al 19-26% Cr, 18-9% Al
Thermal Treatment	
Vacuum heat-treat for 4 h at 1080°C	
Vacuum heat-treat for 4 h at 1080°C and then anneal 1 h in air at 1080°C	
Sputter etched after nitriding for 4 h at 900°C	
None	
Pt Underlayer Thicknesses	
0, 5, and 12.5 μm	
Substrate Alloys	
Mar-M-509, X-40, In-792, and In-738 C	

(a) A value of 27-29% Cr, for example, signifies that the composition gradient was 27 wt% at the base of the deposit (the substrate interface) and increased to 29 wt% at the outer surface of the coating.

Twenty-nine sputter-coated pins and three PVD control samples were tested by L. F. Aprigliano at the Annapolis Naval Ship Research and Development Center (NSRDC). The 500-h test was conducted in a low-velocity, atmospheric pressure burner rig operated on marine diesel fuel containing 2% sulfur (Aprigliano 1980). An aggressive, low-temperature, hot corrosion environment was induced by adding 10-ppm salt concentrations to the inlet air. During the test, the samples were cycled from an operating temperature of 677°C (1250°F) to room temperature at 24-h intervals.

Another set of 18 sputter-coated pins and two PVD control samples were tested by Nicholls and Hancock (1981) at the Cranfield Institute of Technology, Bedford, England. The 100-h test was conducted in a burner rig modified to operate on solvent refined coal (SRC-II) fuel at 750°C. An extremely corrosive vanadate attack of the coatings and massive erosion produced by excessive coking were observed. During the test, the samples were cycled to room temperature every 2 h.

Four high-chromium CoCrAlY coatings were tested for 42 h in a Rolls Royce Olympus C turbine operated on commercially available residual heating fuel. Blade temperatures ranged from 500 to 840°C. Each In-738 turbine blade was first coated with a 5-μm Pt underlayer. The CoCrAlY coating was graded such that the chromium composition was 48 wt% at the coating surface and decreased to 43 wt% at the coating/substrate interface. The aluminum composition was ~8 wt%. Three of the blades were preoxidized for 1 h at 1080°C in air before the test.

A burner rig facility was also assembled at PNL to provide the CZD Program with a dedicated system for alternative fuels testing. Unfortunately, the program was terminated just as the system became operational and preliminary tests with Exxon Donor Solvent, a coal-derived liquid fuel, had been completed.

RESULTS AND DISCUSSION

Results of the NSRDC, Cranfield Institute, and Rolls Royce turbine blade tests are presented in this section. Characterization data on the coatings are also presented.

Coating Characterization

A variety of samples were prepared for testing in different combustion atmospheres. It was expected that a tabulation of test data would evolve that would correlate the corrosion resistance of a CoCrAlY coating in various environments with certain design parameters. As alternative fuels are introduced into service, their actual combustion and corrosive properties could be determined and the CZD-developed data file could be referenced to provide critical materials performance information under similar conditions.

The sputtered coatings prepared for this task were all modifications of a CoCrAlY (23 wt% Cr, 9 wt% Al) coating. Several major variations in the composition were made to study the effects of chromium and aluminum concentration on corrosion behavior. These elements were distributed either homogeneously or with a gradation through the coating thickness. The selection of the composition and, to a lesser extent, the distribution of the individual elements are especially important for coatings used at temperatures below 850°C. In this regime, even small changes in the Cr and Al concentrations will significantly alter the composition of the scales that form and will dramatically affect the corrosion resistance of the deposit.

Coating/substrate interdiffusion was also addressed because of its major effect on corrosion resistance. Typically, a coating becomes depleted in aluminum because of diffusion into the substrate. This diffusion can greatly reduce the life of a coating. Alloy additions made to the substrates, especially Mo or Ti, can also diffuse to the coating surface where they chemically accelerate the corrosive attack. In an attempt to reduce these effects, many of the samples were prepared with a Pt underlayer that separated the substrate and the coating. It was believed that this underlayer would restrict the mobility of selected elements by forming intermetallic compounds (for example, PtAl) and thereby extend the long-term corrosion resistance of the coating. Coatings with graded platinum additions were also prepared to establish whether other distributions might be better. Different substrate materials were tested to assess the problem and to identify those effects that were related to specific substrates.

The as-deposited CoCrAlY deposits were dense, defect-free coatings composed of a fine (submicron) distribution of δ-Co and βAl-Co phases. Following heat treatment at 1080°C for 4 h, grain growth resulted in a coarser two-phase structure with average grain sizes of 4 to 6 μm. An example of the heat-treated microstructure is shown in Figure 3. The metallography of the pretest coatings is presented in more detail in Patten, Moss, and Hays (1980).

Annapolis NSRDC Burner Rig Test

The Annapolis burner rig test provided an aggressive, low-temperature, hot corrosion environment for evaluating the samples. Following the test, the

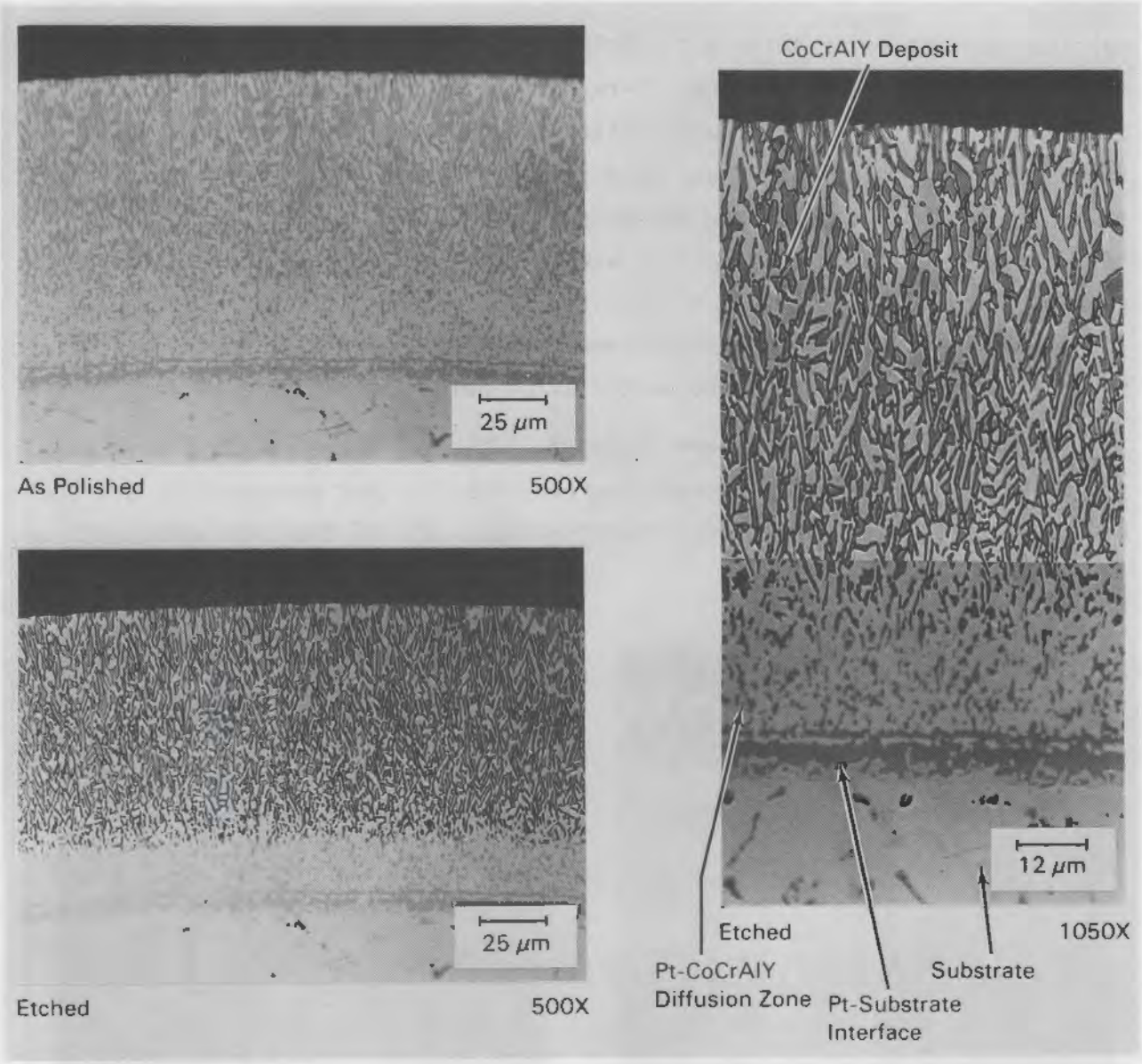

FIGURE 3. CoCrAlY Coating Sputter Deposited onto Sputtered Platinum Underlayer. The substrate is a 1/8-in. diameter In-792 pin. The chromium content of the CoCrAlY is graded from 25% at the interface to 30% at the outer surface. The deposit was heat-treated at 1080°C for 4 h.

upper portion of the surface of each test pin was examined by Auger electron spectroscopy and x-ray photoelectron spectroscopy. The pins were almost completely covered with Na_2SO_4, $CaSO_4$, and mixed silicates; and only trace signals of sulfides and oxides were observed. A subsequent study using SEM equipped with EDX showed that the oxide scale was covered by a heavy deposit of sodium,

calcium, and magnesium sulfates; calcium and magnesium silicates; potassium sulfate; and potassium chloride. X-ray diffraction confirmed the presence of Na_2SO_4 and the existence of oxide spinels, either $CoAl_2O_4$ or Co_2CrO_4. Following a water wash of the surface, only the oxide scale and oxide particles remained. The oxide contained phosphorous and silicon (up to 9 wt%) and a small amount of sulfur (typically 1 wt%). Cross sections of the pins were examined; the corrosion product consisted of a dense oxide scale with a localized pitting attack that contained sulfides. The attack was characterized by the lack of a depletion zone in the alloy below the pit (Figure 4).

Burner rig test samples are listed in Table 2. These coatings have been ranked according to post-test metallography results that measured the average and the deepest corrosion product penetrations. All of the pins were sectioned

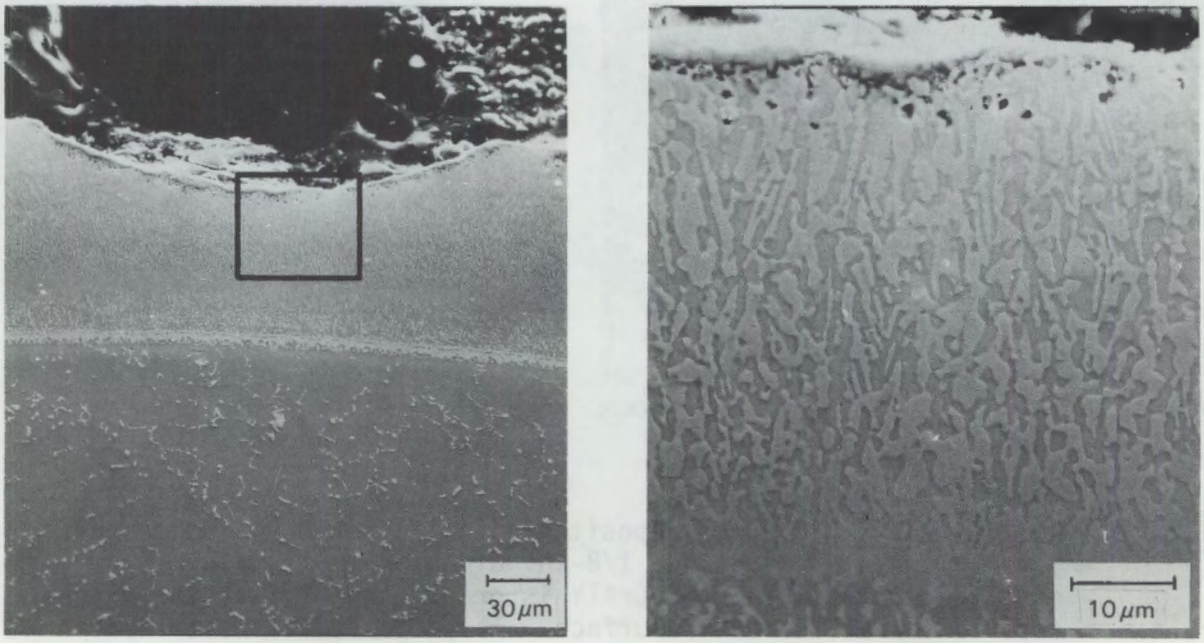

a) Example of Corrosive Attack Observed on Run 2003

b) Enlarged View of Coating Immediately Below Corrosion Pit in Figure 4a

FIGURE 4. Typical Corrosion Pit on Burner Rig Pins Tested at Annapolis NSRDC. The absence of a depletion zone in the underlying metal can be seen in the micrograph on the right.

TABLE 2. Burner Rig Pins Tested at Annapolis NSRDC

Sample	Depth of Attack, μm Average	Maximum	Coating Composition[a]	Thermal Treatment	Pt Underlayer Thickness, μm	Coating Thickness, μm	Substrate Alloy
1021	0	0	27-29% Cr, 6-4% Al	Vacuum heat-treat for 4 h at 1080°C	12.5	120	X-40
5034	0	0	27-29% Cr, 6-4% Al	Vacuum heat-treat for 4 h at 1080°C	0	120	In-792
5005	0	0	27-29% Cr, 6-4% Al	Vacuum heat-treat for 4 h at 1080°C	5	120	In-792
1005	0	0	34% Cr, 3% Al	Vacuum heat-treat for 4 h at 1080°C	5	102	X-40
5014	0	5	35% Cr, 1% Al	Vacuum heat-treat for 4 h at 1080°C	12.5	105	In-792
1048	0	5	12-3-21% Cr, 68-87-17% Pt, 1-0-2% Al	Vacuum heat-treat for 4 h at 1080°C	0	135	X-40
2014	0	5	12-3-21% Cr, 68-87-17% Pt, 1-0-2% Al	Vacuum heat-treat for 4 h at 1080°C	12.5	135	Mar-M-509
2042	0	5	24-30% Cr, 19-3% Al	Vacuum heat-treat for 4 h at 1080°C	0	125	Mar-M-509
2010	0	5	24-30% Cr, 19-3% Al	Vacuum heat-treat for 4 h at 1080°C	12.5	125	Mar-M-509
5003	0	7.5	24-30% Cr, 19-3% Al	Vacuum heat-treat for 4 h at 1080°C	5	125	In-792
2047	0	12.5	34% Cr, 3% Al	Vacuum heat-treat for 4 h at 1080°C	0	102	Mar-M-509
5012	0	25	34% Cr, 3% Al	Vacuum heat-treat for 4 h at 1080°C	12.5	102	In-792
1007	0	25	35% Cr, 1% Al	Vacuum heat-treat for 4 h at 1080°C	5	105	X-40
5037	0	25	35% Cr, 1% Al	Vacuum heat-treat for 4 h at 1080°C	0	105	In-792
1001	2.5	5	19-26% Cr, 18-9% Al	Vacuum heat-treat for 4 h at 1080°C	5	133	X-40
2051	2.5	5	22% Cr, 9% Al	Sputter etched after nitriding for 4 h at 900°C	5	35	Mar-M-509
5007	2.5	20	12-3-21% Cr, 68-87-17% Pt, 1-0-2% Al	Vacuum heat-treat for 4 h at 1080°C	12.5	135	In-792
1040	2.5	23	19-26% Cr, 18-9% Al	Vacuum heat-treat for 4 h at 1080°C	0	133	X-40
2035	5	5	22% Cr, 9% Al	Sputter etched after nitriding for 4 h at 900°C	0	35	Mar-M-509
2054	5	7.5	32-34% Cr, 9% Al	Sputter etched after nitriding for 4 h at 900°C	5	175	Mar-M-509
2031	5	10	30% Cr, 9.5% Al	Vacuum heat-treat for 4 h at 1080°C	0	150	Mar-M-509
2027	5	12.5	33% Cr, 9.4% Al	Vacuum heat-treat for 4 h at 1080°C	0	163	Mar-M-509
2018	5	15	25-30% Cr, 9-8% Al	Vacuum heat-treat for 4 h at 1080°C	0	115	Mar-M-509
1019	5	137	19-26% Cr, 18-9% Al	Vacuum heat-treat for 4 h at 1080°C	12.5	133	X-40
2038[b]	5	135	23% Cr, 9% Al	Heat-treat for 2 h at 1052°C	0	88	Mar-M-509
5027	7.5	220	25-30% Cr, 9-8% Al	None	0	175	In-792
1037	10	10	25-30% Cr, 9-8% Al	None	0	175	X-40
2020	10	65	25-30% Cr, 9-8% Al	Vacuum heat-treat for 4 h at 1080°C	0	138	Mar-M-509
2001	12.5	113	25-30% Cr, 9-8% Al	Vacuum heat-treat for 4 h at 1080°C	5	117	Mar-M-509
2003	12.5	135	25-30% Cr, 9-8% Al	Vacuum heat-treat for 4 h at 1080°C	5	138	Mar-M-509
2058[b]	12.5	138	23% Cr, 9% Al	Heat-treat for 2 h at 1052°C	5	88	Mar-M-509
DTSNRDC[c]	23	275	24% Cr	Heat-treat for 2 h at 1052°C	0	125	Rene 80

(a) A value of 27-29% Cr, for example, signifies that the composition gradient was 27 wt% at the base of the deposit (the substrate interface) and increased to 29 wt% at the outer surface of the coating.
(b) PVD control coating by Airco-Temescal, Berkeley, California.
(c) PVD control coating by NSRDC, Annapolis, Maryland.

at three locations for metallographic examination: 6.35 mm from the top, 6.35 mm from the test carousel, and in the middle of the exposed 22-mm test length. If a localized area of corrosion would have been missed by these sectioning locations, they were modified to include that area. For each sample, the depth of corrosion attack measurements were made every 20° around the circumference of each of the three cross sections. These 54 measurements were averaged to yield an average depth of attack for each coating. The maximum observed depth of attack found on any of the cross sections was also recorded.

Analysis of the depth of attack data showed that composition was the dominant factor in determining the corrosion resistance of the coatings. The lack of redundancy in the samples made it impossible to determine whether the use of different substrate materials or the deposition of a platinum underlayer had minor effects on coating performance. However, it was clear that these effects were very small when compared with the effect of coating composition. Depth of attack results are summarized in Table 3 for the six general types of

TABLE 3. Coating Composition Types for Annapolis Burner Rig Test Results

Group	Coating Composition[a]	Depth of Attack, μm	
		Average	Maximum
I	27-29% Cr, 6-4% Al	0	0
II	24-30% Cr, 19-3% Al	0	8
III	12-3-21% Cr, 2% Al, 68-87-17% Pt	0	20
IV	34% Cr, 3% Al 0	25	
V	19-26% Cr, 18-9% Al	3	120
VI	28% ±5% Cr, 9% Al	4.5	135
VII	25-30% Cr, 9-8% Al	10	220
VIII	PVD control specimens:		
	2 with 23% Cr, 9% Al	9	140
	1 with 24% Cr, 11% Al	23	275

(a) See footnote (a) on Table 2, p. 13.

coating compositions that were tested. In general, the sputtered coatings were superior to similar control PVD coatings. Samples with a low surface concentration of aluminum (1 to 4 wt% Al) were more resistant to the type of hot corrosion experienced in this test than samples with 8 to 11 wt% Al at the coating surface. Excellent corrosion resistance was obtained from the CoCrAlY coatings that had a starting surface composition of 29 wt% Cr, 4 wt% Al, 1.2 wt% Y, and the balance as cobalt (see Samples 1021, 5034, and 5005). This coating is shown in the as-sputtered condition in Figure 5. The graded Pt-CoCrAlY samples were also very corrosion resistant (see Samples 1048, 2014, and 5007). These coatings, shown in Figure 6, contained a platinum gradient that peaked at 90% near the center of the coating thickness and then decreased to 10% at the coating surface. The scale that formed on these samples was a mixed Cr-Al-Co oxide that contained no platinum.

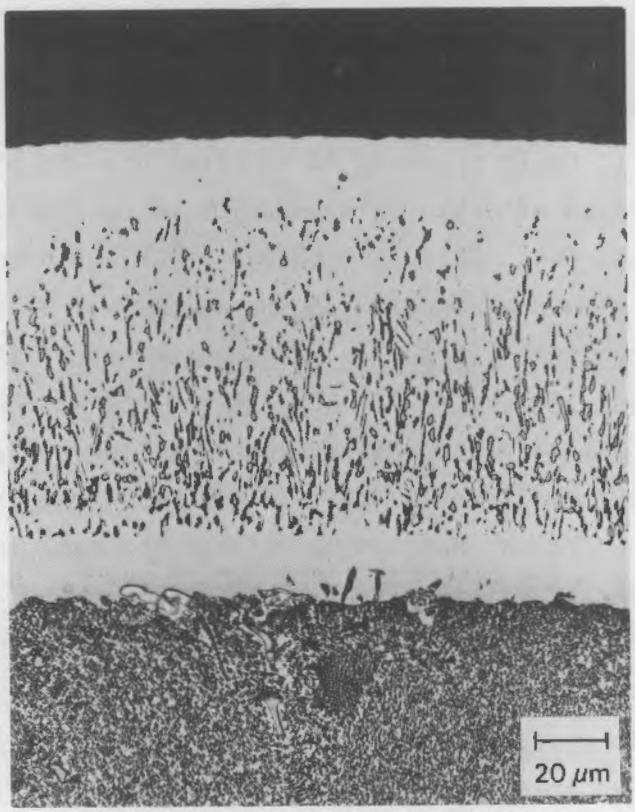

FIGURE 5. Optical Micrograph Showing a Cross Section of a Graded 27-29% Cr, 6-4% Al Coating. The coating was heat-treated at 1080°C for 4 h and then polished and etched.

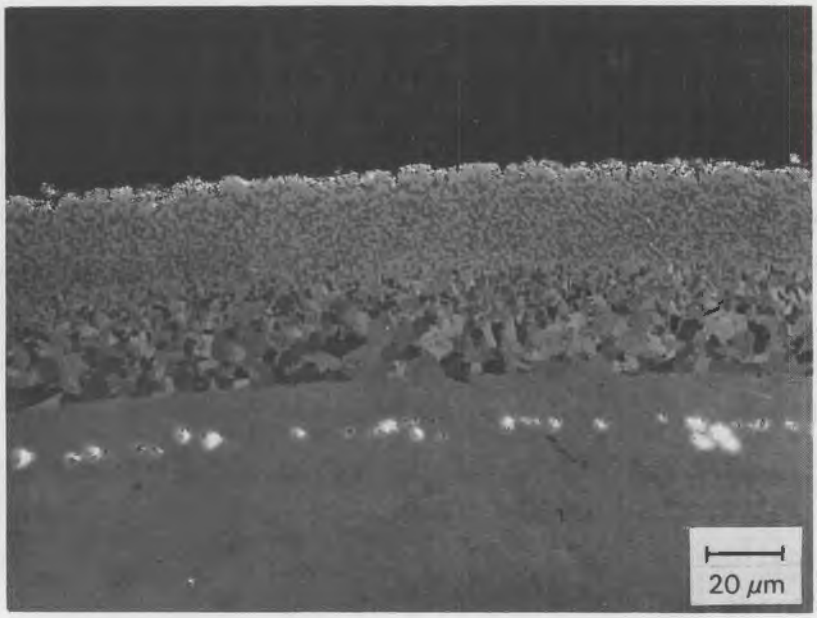

FIGURE 6. Optical Micrograph Showing a Cross Section of a Graded Pt-CoCrAlY Coating After Burner Rig Test

A gradient in the aluminum composition that increased its concentration as a function of coating depth appeared to be beneficial in minimizing the occurrence of deep localized attack. This behavior was dramatized by the Group II coatings (see Samples 2042, 2010, and 5003), which contained a concentration gradient where the aluminum composition increased from 3% to 19% as a function of depth into the coating (Figure 7). Homogenization of this coating occurred during the 500-h test and eventually brought the coating composition to a uniform 20% Cr and 15% Al; i.e., during the test, the surface composition increased gradually from 3% to 15% Al. In general, test results showed that the graded coating performed better than either the homogeneous 3% Al samples, which represented the starting surface composition of the graded coating, or the homogeneous 9% Al samples, which represented the surface composition of the graded coating midway through the test (see Samples 1005, 2047, 5012, 2051, 2035, and 2054). It appeared that a composition gradient in which the aluminum content was increased into the coating thickness was beneficial.

A gradient in the chromium concentration that decreased the chromium content into the coating thickness was detrimental to overall coating corrosion

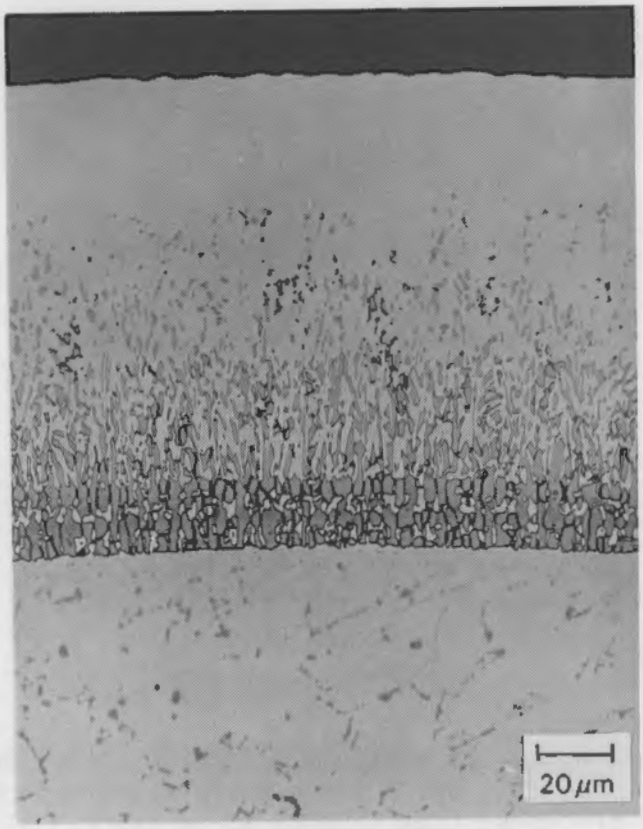

FIGURE 7. Optical Micrograph Showing a Cross Section of a Graded 24-30% Cr, 19-3% Al Coating. The deposit was heat-treated and then polished and etched.

resistance. This behavior was demonstrated by the Group VII coating (see Table 3); these coatings were noticeably less resistant to the low-temperature, hot corrosion attack than the homogeneous Group VI coatings.

Interdiffusion between the coating, the substrate pins, and the platinum underlayers was studied using SEM. Composition profiles across the coating showed that by the conclusion of the 500-h test substrate alloying elements (in particular, Ta, W, and Ni) had permeated through the coating thickness (~130 μm) at a concentration of about 1%. The presence of a platinum underlayer did not affect the diffusion of these three elements. By the conclusion of the 500-h test at 677°C, the platinum underlayers were 45 μm wide and platinum was presented in the CoCrAlY as a separate phase that was rich in aluminum and titanium (see Figure 8). After 500 h at 677°C, very little aluminum had

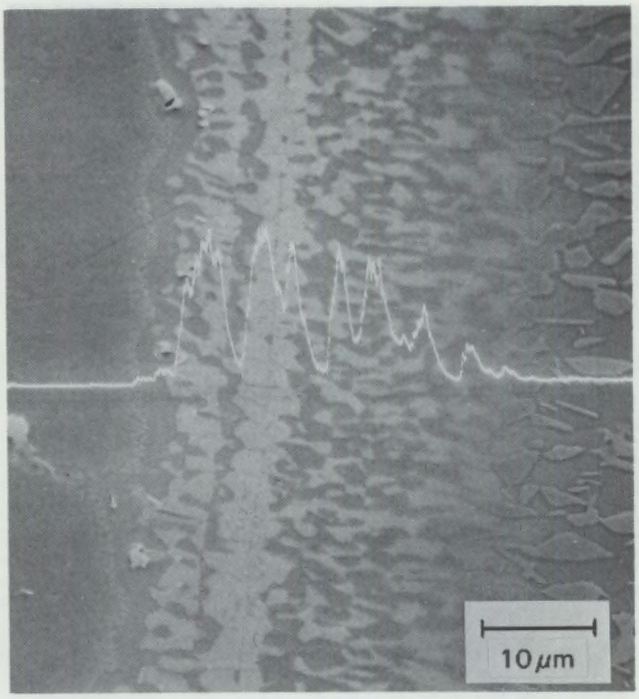

FIGURE 8. SEM Micrograph of Platinum Underlayer After 500-h Burner Rig Test. The line trace shows the platinum concentration; the layer broadened from 5 μm to 33 μm thick. Aluminum and titanium are concentrated in the platinum-rich phase.

diffused out of the coating and into the substrate. In this study, the presence of a platinum underlayer actually accelerated aluminum depletion of the coating. The aluminum diffused rapidly to the platinum-rich phase. However, the long-term effect of the platinum underlayer on the loss of aluminum from the coating at much longer times or higher temperatures was not established.

Titanium and molybdenum are superalloy additions made to In-792 that are believed to aggravate the hot corrosion of alloys if they are present at the surface (Goebel, Pettit, and Goward 1973). Therefore, it is important that coating designs minimize the outward diffusion of these substrate elements through a coating. In this study, the titanium preferentially segregated to the platinum-rich phase. Thus, the platinum underlayer might be expected to have long-term significance on coating performance if it retards titanium diffusion by forming an intermetallic phase. Regrettably, in the present study the time was too short and the temperature too low to test this hypothesis. Neither molybdenum nor titanium had diffused appreciably in any of the samples,

which may be the reason the depth of attack did not show any significant dependence on the choice of substrate or the presence of platinum diffusion barriers.

Cranfield Institute Burner Rig Test with SRC-II

Testing at the Cranfield Institute of Technology provided valuable experience on alloy erosion/corrosion in coal-derived liquid combustion environments. The test was performed using an SRC-II blend of 2.9 parts middle distillate with 1 part heavy distillate. Specimen temperature was held at 750°C for 100 h. Because considerable coke deposits built up during the test, the combustor was shut down and stripped at 2-h intervals to remove the deposits. Even so, chunks of carbon up to 2 cm in diameter were collected from the exhaust tube during the test. A high vanadium content in the fuel dominated the character of the corrosive attack.

Twenty pins with CoCrAlY overlay coatings were tested at Cranfield: 18 coatings were sputter deposited at PNL and the other two were prepared by EB-PVD at Airco-Temescal. Metallography and corrosion analysis were performed at Cranfield. The results are reported in detail by Nicholls and Hancock (1981). The results of the metallography are reproduced in Tables 4 and 5; the coatings are ranked according to the measured depth of corrosive attack. It should be noted that the coating variety in these tests was much less diverse than that tested at Annapolis; coatings tested at Cranfield were the same as those that fell in the lower half of the Annapolis ranking. Comparison of test results from both runs suggests that the SRC-II test was a more severe environment. Interestingly, a comparison of identical pins tested in both experiments showed the ranking of pins to be exactly reversed. Since the combustion atmospheres were very different and different types of attack dominated in the respective tests, this is not surprising; however, it does demonstrate the importance of matching a coating to the corrosive environment.

In the Cranfield tests, the PVD coatings were the most resistant, with an average depth of attack of 8 μm. The sputtered coatings showed generally poorer resistance, although those with compositions similar to the PVD coatings were extremely thin, which may have had a detrimental effect on their corrosion resistance. The coatings with a composition gradient in the chromium content

TABLE 4. Burner Rig Pins Tested at Cranfield Institute

Sample	Depth of Attack, μm		Coating Composition[a]	Thermal Treatment	Pt Underlayer Thickness, μm	Coating Thickness, μm	Substrate Alloy
	Average	Maximum					
2039[b]	6	13	23% Cr, 9% Al	Not known	0	90	In-792
2008	8	36	25-35% Cr, 10-8% Al	Vacuum heat-treat for 4 h at 1080°C	5	180	Mar-M-509
2019	8.5	20	25-30% Cr, 10-8% Al	Vacuum heat-treat for 4 h at 1080°C	0	115	Mar-M-509
2059[b]	9	16	23% Cr, 9% Al	Not known	5	90	In-792
2024	12	20.5	25-35% Cr, 10-8% Al	Vacuum heat-treat for 4 h at 1080°C and 1 h in air at 1000°C	0	180	Mar-M-509
2022	13	26.5	24-33% Cr, 10-8% Al	Vacuum heat-treat for 4 h at 1080°C	0	105	Mar-M-509
2002	14	27	25-30% Cr, 10-8% Al	Vacuum heat-treat for 4 h at 1080°C	5	115	Mar-M-509
2021	14.5	24.5	25-30% Cr, 10-8% Al	Vacuum heat-treat for 4 h at 1080°C	0	150	Mar-M-509
2036	15	21.5	23% Cr, 10% Al	Sputter etched after 4 h at 900°C	0	20	Mar-M-509
5028	16	28.5	25-35% Cr, 10-8% Al	None	0	180	In-792
2004	17.5	28.5	25-30% Cr, 10-8% Al	Vacuum heat-treat for 4 h at 1080°C	5	140	Mar-M-509
2052	18	26.5	23% Cr, 10% Al	Sputter etched after nitriding for 4 h at 900°C	5	20	Mar-M-509
2006	18.5	31	24-33% Cr, 10-8% Al	Vacuum heat-treat for 4 h at 1080°C	5	105	Mar-M-509
2007	19	31	25-35% Cr, 10-8% Al	Vacuum heat-treat for 4 h at 1080°C	5	180	Mar-M-509
2056	21	37	33% Cr, 9% Al	Sputter etched after nitriding for 4 h at 900°C	5	180	Mar-M-509
1038	24.5	50	25-35% Cr, 10-8% Al	None	0	180	X-40
2029	29	43	33% Cr, 9% Al	Vacuum heat-treat for 4 h at 1080°C	0	165	Mar-M-509
2037	30	44	30% Cr, 10% Al	Vacuum heat-treat for 4 h at 1080°C	0	150	Mar-M-509
2028	30	55.5	33% Cr, 9% Al	Vacuum heat-treat for 4 h at 1080°C	0	165	Mar-M-509
2053	32	52	30% Cr, 10% Al	Vacuum heat-treat for 4 h at 1080°C	0	150	Mar-M-509

(a) See footnote (a) on Table 2, p. 13.
(b) PVD control specimen by Airco-Temescal, Berkeley, California.

TABLE 5. Coating Composition Types for Cranfield SRC-II Test Results

Group	Coating Composition[a]	Depth of Attack, μm	
		Average	Maximum
A	2 EB-PVD control specimens: 23% Cr, 10% Al 8	16	
B	25-33% ±3% Cr, 10% Al	15	50
C	23% Cr, 10% Al 16.5	27	
D	32% ±2% Cr, 10% Al	28.4	56

(a) See footnote (a) on Table 2, p. 13.

displayed superior corrosion resistance compared with homogeneous coatings having compositions at either extreme (see Table 5, Group B versus C and D). A small but real difference in corrosive attack was observed between coatings with and without the platinum underlayer. Coatings with the underlayer were slightly less resistant when all of the other coating parameters were the same (Figure 9).

Rolls Royce Engine Test with Residual Fuel

Four turbine blades were tested for 42 h in a Rolls Royce Olympus C engine operated at 1067°C (outlet temperature) using residual fuels (Table 6). The engine was started with diesel fuel and then switched over to a residual fuel for 26.5 h; the engine was returned to diesel fuel prior to shutdown. The residual fuel was a blend of Bunker C and lighter fractions to achieve a viscosity of 220 Redwood secs. The original sodium level of 32 ppm was reduced to less than 0.5 ppm by fuel washing. Petrolite K1-59 was added to the fuel to inhibit the high vanadium content (50 ppm). The sulfur content in the blend was 2.5 wt%. Blade temperatures varied from 830°C at the leading and trailing edges to 500°C near the root.

Each of the blades was first coated with a 5-μm Pt underlayer and then uniformly covered with a 145-μm graded CoCrAlY coating (43-48% Cr, 8-7% Al). Three of the blades were preoxidized for 1 h at 1080°C in air before the test. None of the blades showed any significant attack, although the brevity

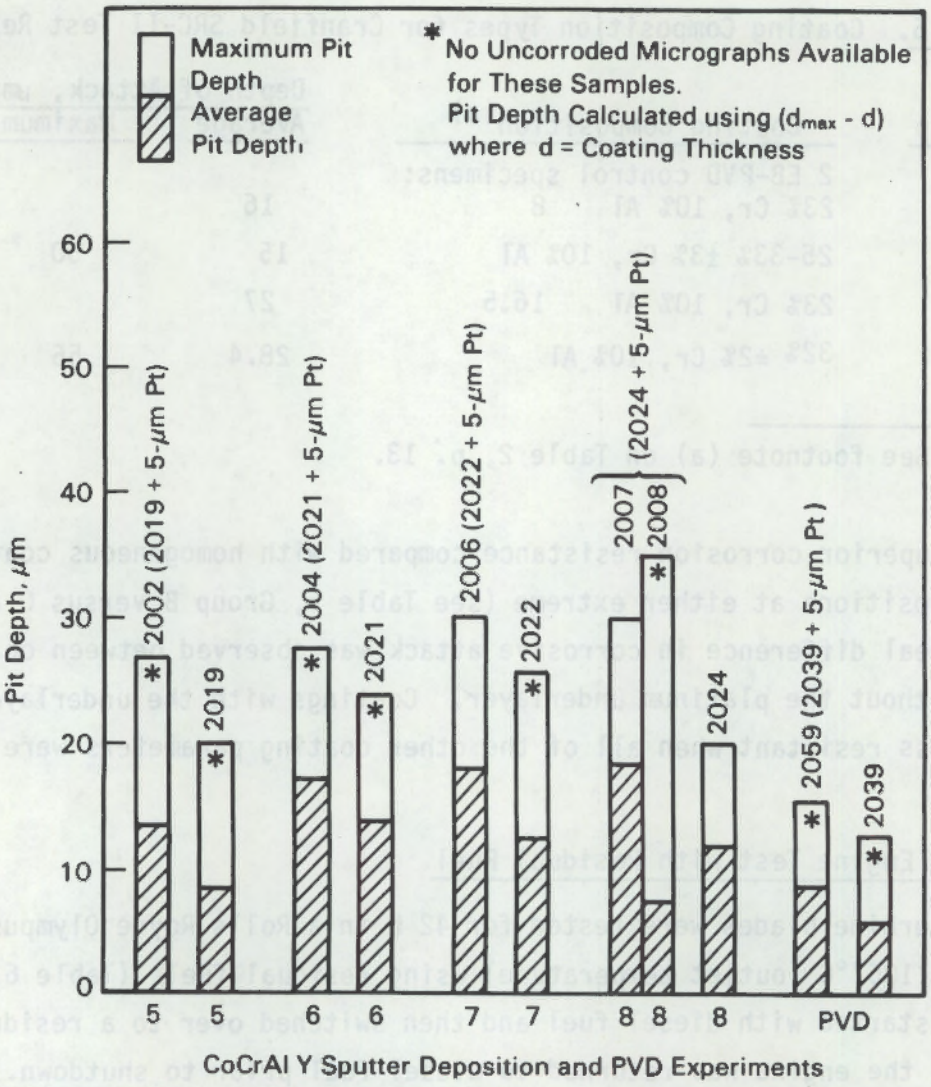

FIGURE 9. Comparison of Corrosion Attack for a Variety of Sputtered, Graded CoCrAlY, and PVD CoCrAlY Coatings With and Without Platinum Underlayers. The presence of a 5-μm underlayer resulted in a slightly greater attack (Nicholls and Hancock 1981).

of the test precluded any major conclusions. The leading edge of a preoxidized blade and a blade with no pretreatment are compared in Figures 10 and 11. A protective Cr_2O_3 scale formed on both samples. The peppered appearance of the preoxidized sample is a result of internal oxidization and precipitation of Al_2O_3 during the oxidation pretreatment.

TABLE 6. Rolls Royce Turbine Blade Coating Test Results

Blade	Coating Composition[a]	Thermal Treatment	Pt Underlayer Thickness, μm	Coating Thickness, μm	Substrate Alloy
23	43-48% Cr, 8-7% Al	Sputter etched after nitriding at 900°C and 1 h at 1080°C in air	5	150	In-738 C
25	43-48% Cr, 8-7% Al	Sputter etched after nitriding at 900°C and 1 h at 1080°C in air	5	150	In-738 C
68	43-48% Cr, 8-7% Al	Vacuum heat-treat for 4 h at 1080°C and 1 h at 1080°C in air	5	150	In-738 C
70	43-48% Cr, 8-7% Al	Vacuum heat-treat for 4 h at 1080°C	5	150	In-738 C

(a) See footnote (a) on Table 2, p. 13.

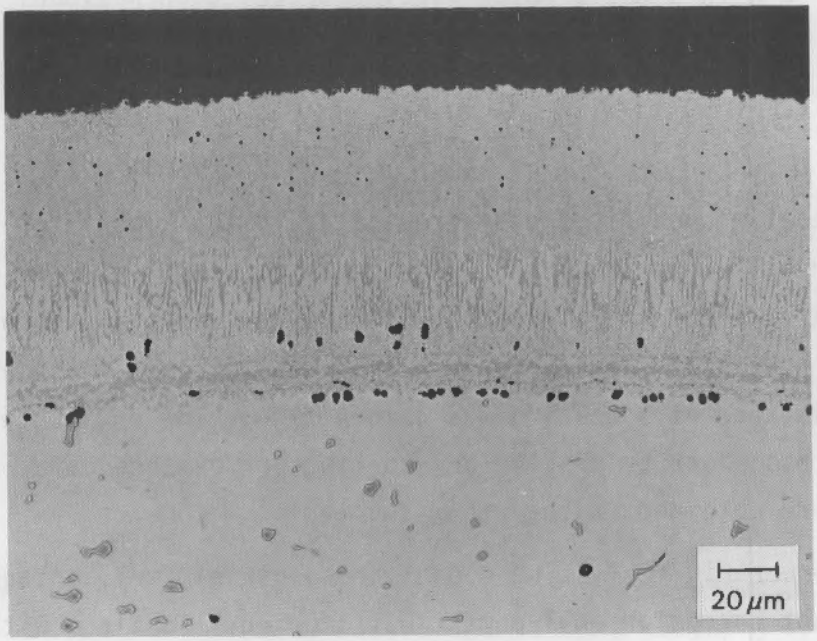

FIGURE 10. Optical Micrograph of CoCrAlY Coating Tested for 42 h in a Rolls Royce Turbine Operated on Residual Fuel

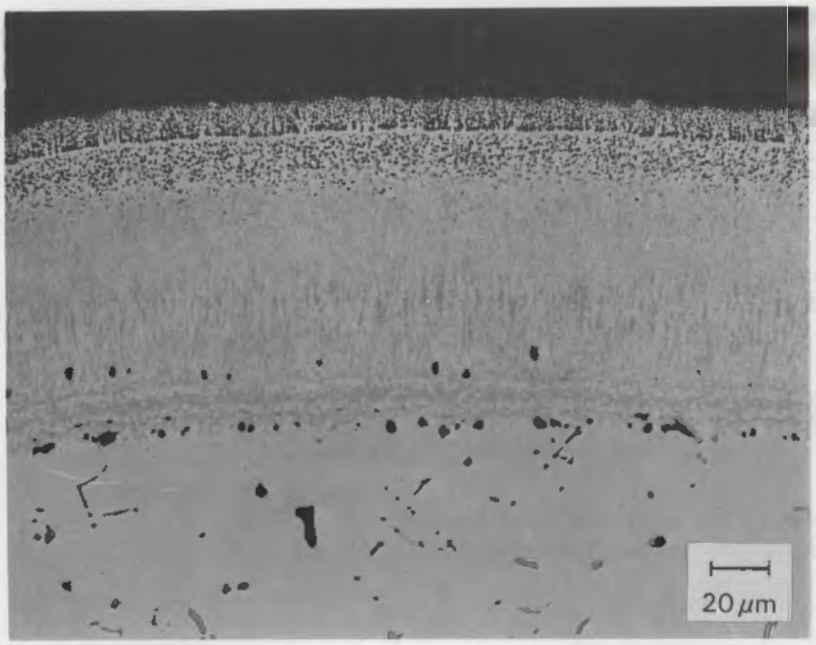

FIGURE 11. Optical Micrograph of Preoxidized CoCrAlY Coating Tested for 42 h in a Rolls Royce Turbine Operated on Residual Fuel. Preoxidation at 1080°C for 1 h before testing resulted in internal oxidation at top of coating.

SUMMARY

CoCrAlY coating modifications were tested in the combustion products of several different fuels: NaCl and S-doped marine diesel, SRC-II coal-derived liquids, and a residual fuel. Coating performance was very dependent on the corrosive environment. The single most important parameter in determining the corrosion resistance of a coating was composition. The engine test with residual fuels was too short to provide any coating performance data, although useful data were obtained in the other two tests.

In the burner rig test using doped marine diesel fuel, an aggressive low-temperature, hot corrosion environment was studied. Coatings with 1) a high chromium surface concentration, 2) a high chromium-to-aluminum ratio at the surface, and 3) a gradient in the aluminum composition that increased the aluminum concentration into the coating thickness improved the corrosion resistance of the coatings. Deposits of CoCrAlY with large additions of platinum also provided good low-temperature protection.

The SRC-II test was an extremely aggressive corrosive attack brought on by the high vanadium content of the fuel. Of the coatings tested, those with a low chromium surface concentration and a chromium composition gradient that increased the chromium composition into the coating thickness improved the corrosion resistance of the coatings.

Both tests indicated that thick platinum underlayers were not effective diffusion barriers. Aluminum and titanium did show a chemical preference for platinum; however, the presence of a platinum underlayer appeared to enhance the diffusion of these species across the substrate/coating interface.

considered to be beneficial in diffusing the sharp discontinuity in modulus and thermal expansion properties that exists at the metal/ceramic interface. The columnar structure in the ceramic regions is considered to be beneficial in accommodating the lateral strains generated near the metal/ceramic interface by permitting expansion and contraction in the gaps between the columns.

Two series of coatings were prepared to study the use of graded transition zones. For both sets of coatings, a 50-μm thick CoCrAlY layer was sputter deposited. The ceramic material (zirconia or alumina) was then co-sputtered with CoCrAlY to produce a broad transition zone with a segmented (columnar) structure. The ceramic composition was gradually increased towards the coating surface. In one case, the grading was continued until a pure ceramic layer was achieved. A thick layer of segmented ceramic was then deposited over the graded material, followed by deposition of a dense (nonsegmented) ceramic layer to act as an impermeable closeout layer. Previous experiments with similar coatings showed that spallation in these coatings occurred by the propagation of cracks in the pure ceramic layer parallel to the deposit surface (Patten et al. 1980). Based on these results, a second group of coatings was prepared in which deposition of the transition zone was stopped before a pure ceramic was obtained. The outer surface composition was ~5% CoCrAlY and 95% ceramic. It was expected that the small concentration of retained metal would make the ceramic coating more ductile, more crack resistant, and more impermeable to combustion products.

Multilayered metal/ceramic composite coatings were also investigated. In this coating design, alternating thin layers of metal and ceramic were deposited. It was expected that the stresses generated by the thermal expansion mismatch would be concentrated in the ductile metal layers or at the ductile metal/ceramic interfaces. By keeping the ceramic layers thin, thermal gradients across any one ceramic layer would be relatively small, reducing the possibility of thermal-shock-induced cracking or spalling. The metal layers made were thick enough to provide ductility and to accommodate the mismatch in thermal expansion. A columnar grain structure was deposited in the thin

CERAMIC COATING DEVELOPMENT

The durability of directly fired heat engines operating on minimally processed liquid fuels is expected to depend on the hot corrosion and erosion resistance of the combustion components. Several ceramic coating materials have been shown to have excellent resistance to aggressive hot corrosion environments (McKee and Siemers 198D) (Ruckle 1980) (Dapkunas and Clarke 1974) and are therefore promising as protective coatings. However, retaining adherence of these coatings to metallic components has been difficult.

The adherence problem arises from: 1) the inability of brittle ceramic materials (particularly dense coatings) to accommodate modulus and thermal expansion mismatches with metal substrates and 2) the entrainment of corrosion products or condensates in coating porosity, which stresses the surrounding ceramic coating and induces spallation during subsequent thermal cycling. To date, the most effective way to improve ceramic adherence has been to introduce porosity into the coating. The pores afford the coating some toughness by blunting crack propagation. However, porous coatings are compromised when used in engines operated on low-grade fuels with high impurity concentrations. These impurities produce liquid and solid combustion products that can collect in the coating porosity; these combustion products stress the coatings (Bratton, Lau, and Lee 1980) and leach phase-stabilizing elements from the coatings (McKee et al. 1979) (Barkalow and Pettit 1979) (Hodge, Miller, and Gedwill 1980). Coating spallation then results during subsequent thermal cycles. To minimize entrainment of these contaminants, a dense and, if possible, self-healing outer layer is required.

The need for a ceramic coating that is both adherent to a metal substrate and impermeable to liquid and gaseous combustion products has long been recognized at PNL (Fairbanks et al. 1975). For the past 8 years, a number of coating design approaches have been examined in an effort to obtain an adherent and impervious ceramic deposit (Bayne et al. 1979) (Patten et al. 1979b). This work identified that a segmented ceramic structure and a graded transition zon between metal and ceramic layers are useful techniques for improving coating adherence, at least at temperatures below 500°C. A broad transition zone is

ceramic layers to promote microcracking at grain boundaries and to discourage cracking in the deposit plane. Ideally, each columnar ceramic grain would be separated from neighboring ceramic grains but attached to metal layers at each end.

EXPERIMENTAL PROCEDURES

All coatings were prepared in the PNL-developed sputter deposition system shown in Figure 12. This system is capable of sputtering from two independent, opposing 23-cm diameter planar targets (one MCrAlY and one ceramic). Each target was covered with a shutter when not in use. Four ceramic materials were investigated: $ZrO_2 \cdot 20Y_2O_3$; $ZrO_2 \cdot 8Y_2O_3$; Al_2O_3; and $Al_2O_3 \cdot 40Cr_2O_3$. Enhanced thermionically supported discharge dc sputtering was used for high-rate deposition (20 μm/h) of the metallic layers. Conventional rf diode or rf-supported discharge techniques were used to deposit the ceramic layers at ~0.4 μm/h. Research-grade krypton was the sputtering gas; a 50-50 mixture of $Kr\text{-}O_2$ was

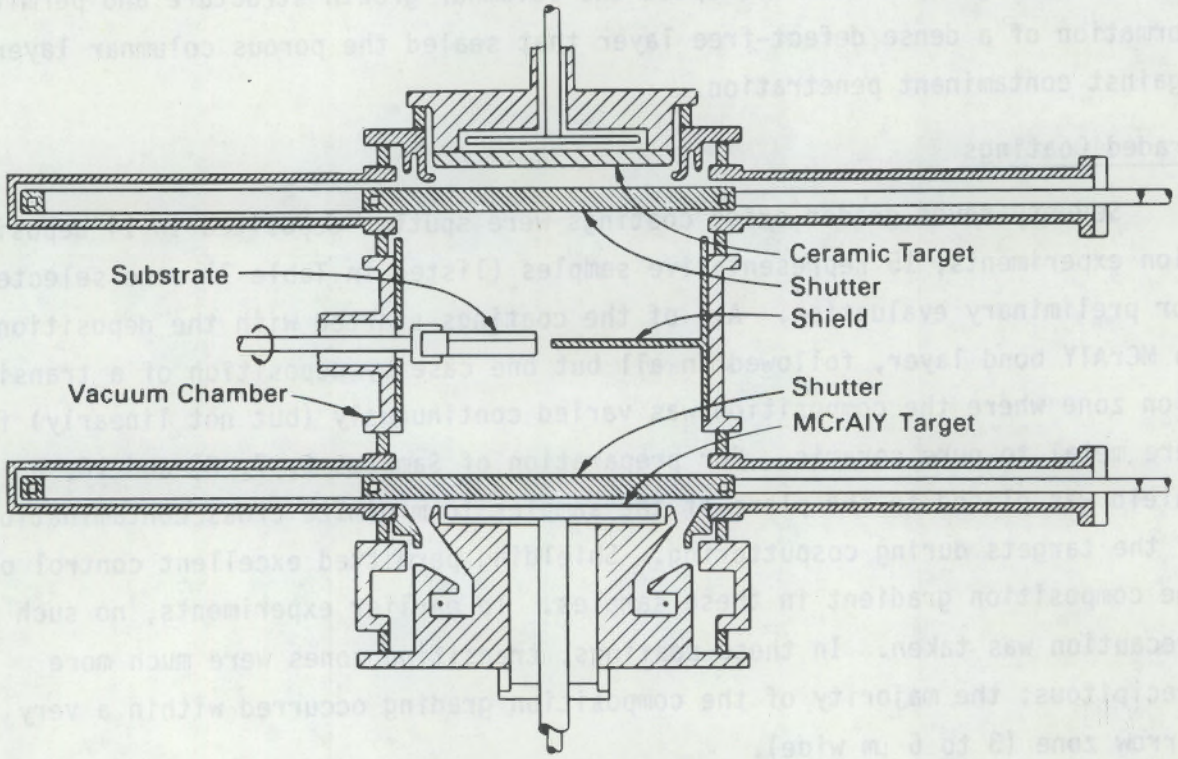

FIGURE 12. Sputtering Chamber Used for Preparation of Ceramic Coatings

used for selected ceramic deposits to help maintain stoichiometry. Graded metal/ceramic layers were prepared by gradually ramping the ceramic power to full power while simultaneously lowering the voltage on the metal target. Typical maximum operating levels were 2 kW rf on the ceramic target and 8.4 kW dc (2.4 kV, 3.5 A) on the alloy target. Substrate temperatures were ~700°C during MCrAlY deposition and ~300°C during ceramic deposition.

The substrates were usually X-40 and In-792 burner rig wedge test specimens (~9 x 10 x 63 mm). Two early experiments used hollow 1.3-mm diameter 304 SS tubes. For each deposition experiment, up to seven burner rig wedge test specimens were positioned in the sputtering chamber midway between the two targets. The substrates were continuously rotated at 24 rpm during deposition to enhance the growth of voids or leaders that develop by a geometric shadowing mechanism (Patten 1979). By selecting sputtering parameters conducive to the formation of coatings with a very large number of leaders perpendicular to the substrate, it was possible to prepare coatings with a pronounced columnar (segmented) structure. Application of a small negative bias voltage to the substrates during deposition disrupted the columnar growth structure and permitted formation of a dense defect-free layer that sealed the porous columnar layer against contaminant penetration.

Graded Coatings

Seventy-seven graded oxide coatings were sputter deposited in 14 deposition experiments; 15 representative samples (listed in Table 7) were selected for preliminary evaluation. All of the coatings started with the deposition of an MCrAlY bond layer, followed in all but one case by deposition of a transition zone where the composition was varied continuously (but not linearly) from pure metal to pure ceramic. For preparation of Samples 6, 7, 8, and 10, a shield was placed in the plane of the samples to minimize cross contamination of the targets during cosputtering. Shielding permitted excellent control of the composition gradient in these samples. In earlier experiments, no such precaution was taken. In these coatings, transition zones were much more precipitous; the majority of the composition grading occurred within a very narrow zone (3 to 6 μm wide).

TABLE 7. Composition of Metal/Ceramic Coatings Tested

Sample	Sputtering Run	Substrate	MCrAlY Bond Layer	Transition Zone[a]	Ceramic Layer
1	WTB-2	304 SS	30-μm NiCrAlY (11% Al)	8-μm dense NiCrAlY/ZrO_2•$20Y_2O_3$	38-μm segmented ZrO_2•$20Y_2O_3$
2	WTB-3	304 SS	30-μm NiCrAlY (11% Al)	16-μm segmented NiCrAlY/ZrO_2•$20Y_2O_3$	38-μm segmented ZrO_2•$20Y_2O_3$
3	MC-13-7	X-40	50-μm CoCrAlY (14% Al)	3-μm segmented CoCrAlY/ZrO_2•$20Y_2O_3$	15-μm segmented/dense ZrO_2•$20Y_2O_3$; O_2 added
4	MC-14-6	X-40	50-μm CoCrAlY (14% Al)	8-μm segmented CoCrAlY/ZrO_2•$20Y_2O_3$	24-μm segmented ZrO_2•$20Y_2O_3$
5	MC-15-5	X-40	50-μm CoCrAlY (14% Al)	3-μm segmented CoCrAlY/ZrO_2•$20Y_2O_3$	24-μm segmented ZrO_2•$20Y_2O_3$
6	MC-23-1	In-792	40-μm CoCrAlY (6% Al)	3-μm segmented CoCrAlY/ZrO_2•$8Y_2O_3$	4-μm segmented/dense ZrO_2•$8Y_2O_3$; O_2 added
7	MC-24-1	In-792	33-μm CoCrAlY (6% Al)	12-μm segmented CoCrAlY/ZrO_2•$8Y_2O_3$	5-μm segmented/dense ZrO_2•$8Y_2O_3$;
8	MC-26-2	In-792	63-μm CoCrAlY (6% Al)	Oxidized CoCrAlY prior to ceramic deposition	4-μm segmented/dense ZrO_2•$8Y_2O_3$; O_2 added
9	MC-27-3	In-792	60-μm CoCrAlY (14% Al)	40-μm segmented CoCrAlY/ZrO_2•$20Y_2O_3$; O_2 added	7-μm segmented/dense ZrO_2•$20Y_2O_3$; O_2 added
10	MC-25-1	In-792	36-μm CoCrAlY (6% Al)	10-μm segmented CoCrAlY/Al_2O_3•$40Cr_2O_3$	5-μm segmented/dense Al_2O_3•$40Cr_2O_3$;
11	MC-27-3	In-792	60-μm CoCrAlY (14% Al)	40-μm segmented CoCrAlY/Al_2O_3; O_2 added	7-μm segmented/dense ZrO_2•$20Y_2O_3$; O_2 added
12	MC-17-7	In-792	50-μm CoCrAlY (14% Al)	20-μm segmented CoCrAlY/Al_2O_3	None
13	MC-18-7	In-792	50-μm CoCrAlY (14% Al)	20-μm segmented CoCrAlY/ZrO_2•$20Y_2O_3$	None
14	MC-19-6	In-792	50-μm CoCrAlY (14% Al)	30-μm segmented CoCrAlY/Al_2O_3; O_2 added	None
15	MC-20-6	In-792	50-μm CoCrAlY (14% Al)	30-μm segmented CoCrAlY/ZrO_2•$20Y_2O_3$; O_2 added	None

(a) The thickness of the transition zone is the area where the composition varies from 10 to 95 wt% zirconia or alumina.

Two types of graded coatings were prepared. In the first group (Samples 1 through 11), the deposition of the graded zone continued until pure ceramic was obtained. The thickness of the transition layer varied from 40 μm in Samples 9 and 11 to 0 μm in Sample 8. A thick pure ceramic layer was then deposited. In most cases, the graded zone was composed of densely packed columns (0.1-μm diameter) that developed by geometric shadowing. This columnar structure continued smoothly into the pure ceramic layer. In many coatings, the last 1 to 2 μm of ceramic was deposited as a dense sealing layer by applying an rf-induced dc bias to the substrate. This bias resulted in ion bombardment of the substrate that disrupted the columnar growth and permitted formation of a dense, defect-free closeout layer. These deposits have been designated by a segmented/dense notation in Table 7.

The second group of coatings (Samples 12 through 15) was prepared with a thick graded zone. Deposition was terminated on these coatings before pure ceramic was obtained. Samples 12 and 14 were prepared with Al_2O_3 as the ceramic material; Samples 13 and 15, with $ZrO_2 \cdot 20Y_2O_3$. These coatings were deposited onto solid In-792 substrates following a trial experiment in which it was found that the hybrid Al_2O_3-CoCrAlY coatings failed to adhere to hollow X-40 substrates.

Microstructure, composition, heat-treatment behavior, and thermal cycle durability were characterized on the samples listed in Table 7. Two sections from each sample were used to prepare metallographic specimens; one in the as-deposited condition and one after an 8-h vacuum heat treatment at 1080°C. Structural and composition studies were performed using an x-ray diffractometer and SEM with EDX. A similar pair of as-sputtered and vacuum heat-treated sections was subjected to a series of ten 10-min thermal cycles at 1000°C. In the first five cycles, the samples were air cooled to 150°C; in later cycles, the samples were quenched into water.

Multilayered Coatings

Four solid In-792 burner rig test pins (0.95-cm diameter) were coated in an early version of the sputtering system. The only differences were the lack

of the central shield and the absence of the shutter covering the ceramic target. A layered deposit was prepared by alternately sputtering from a Ni-50Cr target (operated in a dc triode mode) and then a $ZrO_2 \cdot 20Y_2O_3$ target (operated in an rf diode mode). A Ni-50Cr layer was deposited first, followed by a $ZrO_2 \cdot 20Y_2O_3$ layer, another metal layer, etc., until a total of five metal and four ceramic layers had been deposited. Each layer was 25 μm thick.

A shutter was placed over the metal target when it was not in use to prevent contamination from the ceramic target during rf sputtering. Such contamination would have prevented subsequent dc sputtering from the metal target. A limited degree of composition grading was achieved in the transition area between the metal and ceramic layers. The ZrO_2 deposited in the first 5 μm of ceramic deposition was very high in nickel and chromium. The concentrations of these elements decreased and the zirconium concentration increased as ceramic deposition continued. This behavior was attributed to removal of Ni-Cr contamination from the ZrO_2 target after each Ni-Cr deposition. The pure ZrO_2 layer was ~18 μm thick. In contrast, the transition from the ceramic layer to the next metal layer was very sharp since no similar resputtering step was possible with the metal target.

Metallographic examination indicated that all metal layers were free of growth defects and appeared to be mechanically sound. The ceramic layers were characterized by a high density of growth defects (columnar voids) throughout the thickness of each layer. These voids seemed to have no effect on the growth or structure of the metal layers.

One of the 9.5-mm diameter coated solid pins was also thermally cycled 12 times in air between room temperature and 1100°C using a radiant furnace. Each cycle consisted of ~80 s of heating and ~120 s of cooling. In addition, four similar multilayered coatings were evaluated in a burner rig test conducted at Westinghouse for the National Aeronautics and Space Administration (NASA) (Andersson et al. 1982). Three thermal cycling tests were performed using fuels with different impurity concentrations to evaluate various advanced coating designs for future industrial turbine applications. The four coatings tested were nine-layer deposits of NiCrAlY and $ZrO_2 \cdot 20Y_2O_3$ deposited onto Udimet 720 domed button substrates (13 mm in diameter and 9.5 mm tall).

RESULTS AND DISCUSSION

Three aspects of coating design are discussed in this section: 1) the feasibility of incorporating graded metal-to-ceramic layers to act as compliant transition layers separating the metallic bond layer and the ceramic deposit or as autonomous protective coatings; 2) the potential for using dense closeout layers to extend the life expectancy of porous ceramic deposits exposed to dirty combustion environments; and 3) the possibility of preparing multilayered coatings consisting of alternating metallic and ceramic layers as an alternative to duplex coatings consisting of a ceramic layer deposited over a metallic bonding layer. Test results are presented that identify how each coating design performed under thermal cycling tests in oxidizing environments.

Graded Transition Layers

This section presents the test results of coatings with graded metal-to-ceramic layers. The samples selected for characterization are described in Table 7. All of the coatings started with the sputter deposition of a 50-μm thick MCrAlY layer. The ceramic material (zirconia or alumina) was then cosputtered with MCrAlY to produce a transition zone where the composition was graded from pure metal to nearly pure ceramic. The thickness of the transition layer varied from 0 to 40 μm. In Samples 1 through 11, a thick ceramic layer was sputter deposited over the transition layers. For Specimens 12 through 15, the transition zone deposition was stopped before a pure ceramic was obtained. The outer surfaces of Samples 12 through 15 contained about 5% CoCrAlY. With the exception of Sample 1 and the outermost closeout layers, all of the coatings were sputter deposited with a densely packed columnar structure extending through the coating thickness. A fracture surface perpendicular to the plane of Sample 2 showing this segmented structure is presented in Figure 13.

In the as-deposited condition, the CoCrAlY was a very fine distribution of δ-Co and βAl-Co phases. Ceramic layers of $ZrO_2 \cdot 20Y_2O_3$ and $ZrO_2 \cdot 8Y_2O_3$ were deposited with a cubic crystal structure; Al_2O_3 and $Al_2O_3 \cdot 40Cr_2O_3$ layers were amorphous. Vacuum heat treatments of these coatings at 1080°C for 4 to 8 h produced a series of changes in the microstructures. Recrystallization in the CoCrAlY layer resulted in a much coarser grain structure (Figure 14) and a more ductile fracture behavior after heat treatment. A very fine distribution of

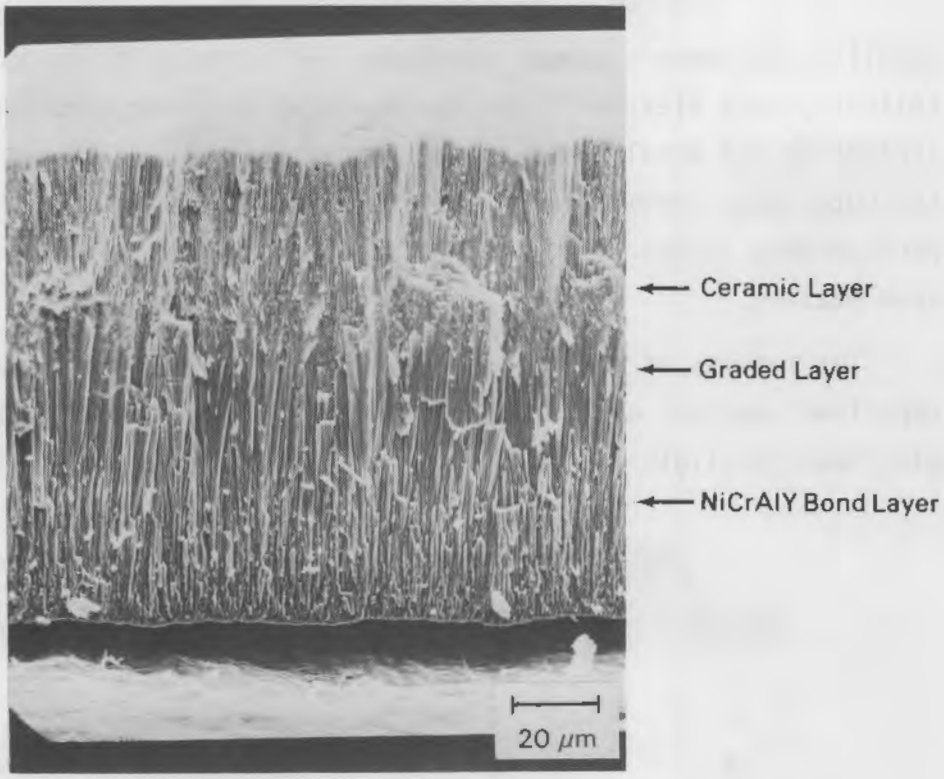

FIGURE 13. SEM Micrograph of Fracture Surface Showing Segmented Structure of Sample 2 in the As-Deposited Condition

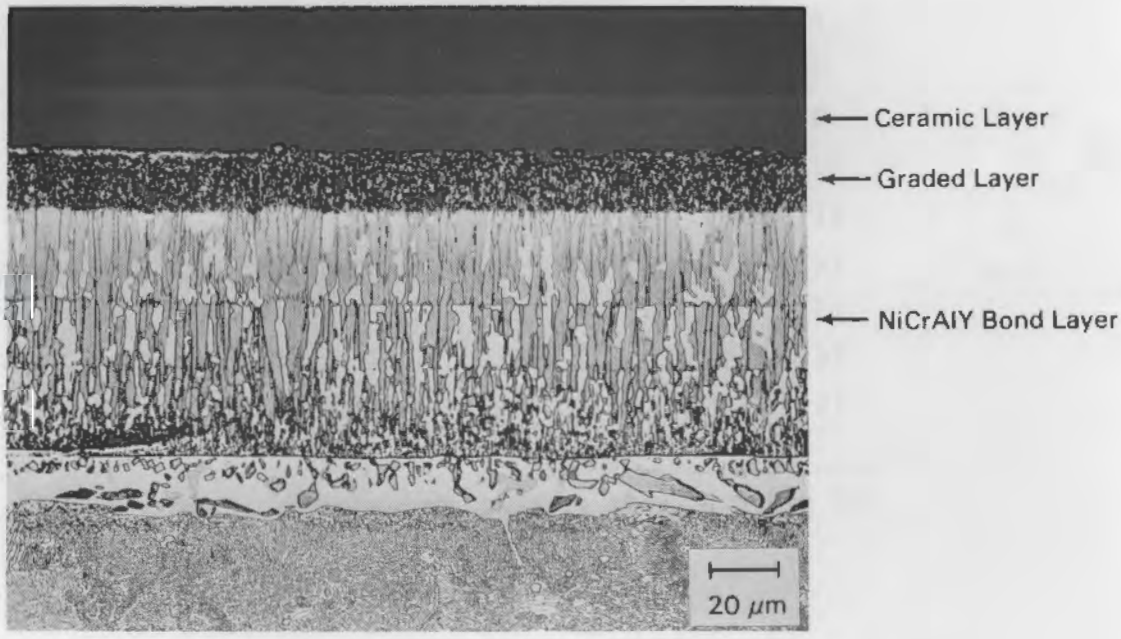

FIGURE 14. Optical Micrograph of Sample 3 Following Heat Treatment at 1080°C. The sample was polished and lightly etched.

metallic and ceramic phases developed in the metal-to-ceramic transition zone. Following heat treatment, the as-deposited columnar structure was no longer present in the metal layer or the transition zone, although it did persist in the pure outer ceramic layer. Brittle fracture behavior was displayed in the pure ceramic layers. The amorphous alumina deposits transformed to δ-alumina upon heating.

The results of the thermal cycling experiment, performed on the as-deposited samples, are presented in Table 8. Prior heat treatment of the samples had a negligible effect on the results of this experiment. Only the

TABLE 8. Results of Thermal Cycling Experiment

Sample	Number of Cycles	Appearance
1	3	80% spalled
2	4	80% spalled
3	10	No spallation or cracking
4	10	20% spalled at radii
5	10	No spallation or cracking
6	10	50% spalled
7	5	95% spalled
8	10	No spalling or cracking
9	3	50% spalled
10	1	100% spalled
11	(a)	
12	3	Severely cracked, 5% spalled
13	2	20% spalled at radii
14	3	Severely cracked
15	2	50% spalled

(a) Never tested; spalled during preparation.

ZrO_2-based ceramic coatings (Samples 3, 5, and 8), which had either very narrow or no transition zones, survived the thermal cycling tests without significant coating spallation or cracking. The failure surfaces of the other eight coatings were examined; the zirconia deposits generally fractured in the graded transition zone, while the alumina coatings spalled by fracture near the base of the pure ceramic layer. This behavior was consistent with the changes in coating microstructure that occurred at elevated temperature.

MCrAlY-$ZrO_2 \cdot Y_2O_3$ Coatings with Graded Transition Layers

In the MCrAlY-$ZrO_2 \cdot Y_2O_3$ samples, the presence of a graded transition layer between the pure metal bond layer and the pure oxide coating increased the spallation of the outer $ZrO_2 \cdot Y_2O_3$ layer. When these samples were annealed at 1080°C, an Al_2O_3-rich phase developed within the graded metal-to-ceramic layer (Figure 15). The composition of this phase was ~50% Al_2O_3, 40% $ZrO_{1.7}$, and 10% Y_2O_3. Its thickness varied roughly with the width of the graded transition layer. This band of alumina was concentrated at a location in the graded zone that originally had a composition of 70% CoCrAlY and 30% $ZrO_2 \cdot Y_2O_3$, i.e., it was clearly located below the pure ceramic layer.

The oxidation of a metallic phase has frequently been associated with the failure of graded coatings. It has always been assumed that the oxidation of the metal generates large internal stresses in the coating and produces spallation. The source of the oxygen has been assumed to be the external atmosphere. In this case, however, the source of the oxygen was identified as being that incorporated in the graded layer at the time of deposition. The coating failure was clearly associated with the thermodynamic instability that exists between the MCrAlY and the ZrO_2, i.e.,

$$2Al + 3/x\ ZrO_2 \rightarrow Al_2O_3 + 3/x\ ZrO_{2-x}\ (0 < x < 0.3 \text{ or } x = 2)$$

The source of the oxygen was positively identified as that deposited in the coating during the sputtering of ZrO_2; a deposit was prepared that sandwiched a graded $ZrO_2 \cdot 20Y_2O_3$-CoCrAlY layer between two CoCrAlY layers. This deposit was

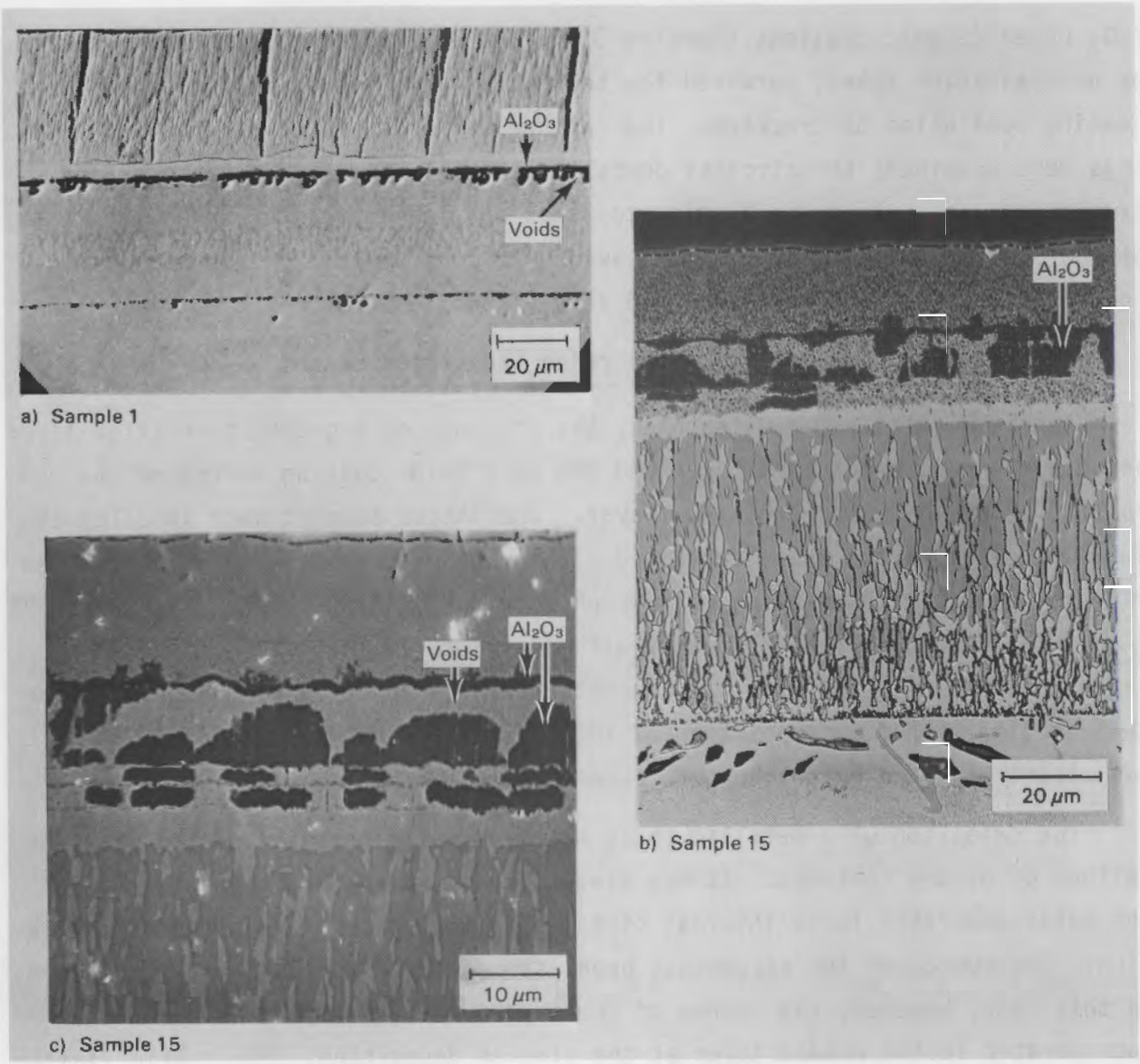

FIGURE 15. Nearly Continuous Alumina Band (dark phase) and Voids Formed in Graded MCrAlY-$ZrO_2 \cdot Y_2O_3$ Layers After Annealing at 1080°C for 8 h

heat-treated at 750°C for 15 min in a vacuum and then cross sectioned. An alumina band at the center of the graded zone was identical to that found in the graded ceramic coatings. This band had formed under high vacuum conditions in a region completely enclosed by unoxidized CoCrAlY, an excellent oxygen barrier. The only source of oxygen was the ZrO_2 that was deposited in the graded layer.

The alumina phase formed in the graded ceramic coatings due to the massive influx of aluminum and oxygen into the middle of the graded region and the expulsion of chromium and cobalt. The source of the aluminum was the MCrAlY layer, while the source of the oxygen was the ZrO_2 that was incorporated into the graded layer at the time of deposition. Composition analysis indicated that the zirconia in the graded region was in a partially reduced state ($ZrO_{1.7}$). As a result of the massive redistribution of oxygen and aluminum in this zone, the metallic phase surrounding the alumina-rich zones developed a large amount of porosity, which weakened this region and made it extremely susceptible to crack propagation.

These same features evolved during thermal cycling experiments. All the thermal cycling failures were associated with the formation of this Al_2O_3 band. Upon cooling, spallation occurred after the first few cycles as cracks propagated along the row of voids and through the zone containing the Al_2O_3 phase (Figure 16).

In an attempt to retard the formation of the alumina band, the concentration of aluminum in the CoCrAlY target was reduced from 14 wt% to 6 wt% to reduce the supply of aluminum. At this composition, the deposit was essentially single-phase δ-Co. Unfortunately, this modification did not reduce the growth of the alumina band or the spallation of the coating. To be effective, it appears that a bond coat containing no aluminum would be required. However, ZrO_2 coatings are quite permeable to oxygen, both by bulk diffusion and by diffusion along the coating porosity. Thus, a major requirement for retaining long-term coating integrity is good high-temperature oxidation resistance of the bond coat, which would be sacrificed if alumina-forming alloys were ruled out as candidate bond coat materials.

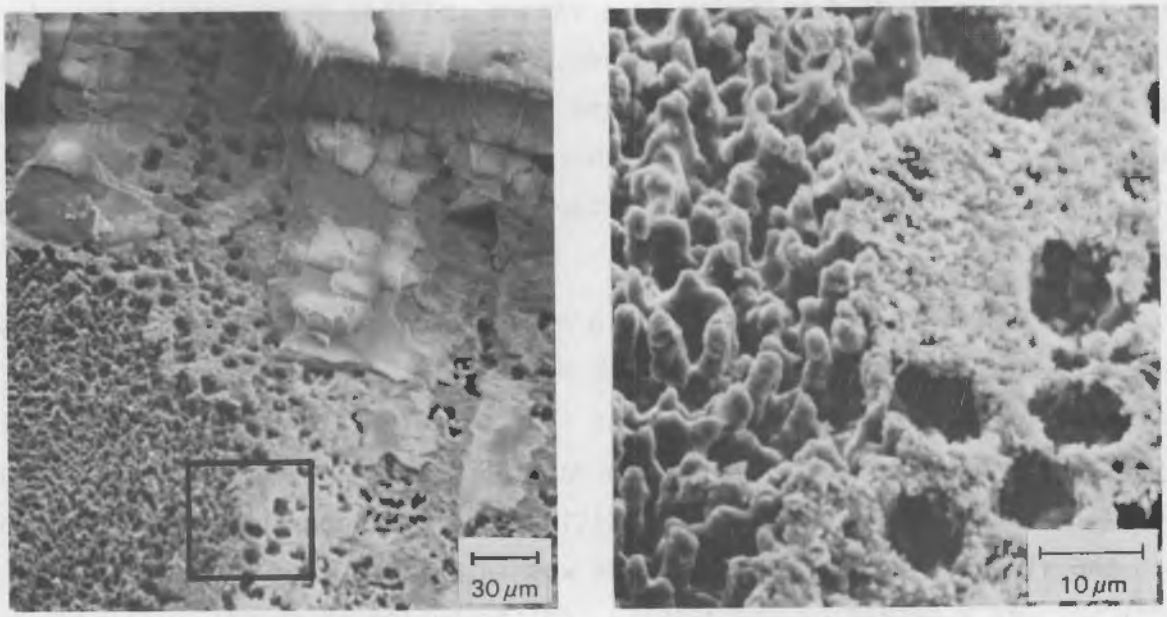

a) Spalled Region of Ceramic Coating

b) Enlarged View of Fracture Surface Showing a Partially Intact Al_2O_3 Layer and the Voids that Formed

FIGURE 16. Fracture Surface of Sample 1 Following Three Thermal Cycles to 950°C. The major mode of failure is by crack propagation through the row of voids and the alumina phase that formed in the graded zone (Figure 15a).

The only parameters that affected the formation of the alumina band were the width of the transition zone and the addition of O_2 to the sputtering gas during deposition of the graded layer. Increasing the width of the graded transition layer or adding oxygen to the plasma during the deposition of that layer increased the amount of alumina formed.

The severity of this interdiffusion problem can be attributed to some unique features that characterize PVD coatings in general and sputtered coatings in particular. First, when metal and oxide phases are co-sputtered, they become mixed on a very fine scale (submicron grain sizes as opposed to 50-μm particle sizes typical of plasma-sprayed coatings). This mixing provides a huge contact area between phases and enhances the kinetics of any favorable reaction. In addition, the substrate surfaces used for PVD coatings are generally quite smooth; this featureless surface is replicated in the coating. In

the present work, this smooth surface resulted in the localization of the Kirkendall voids to one well-defined plane that was highly susceptible to crack propagation. Because of this localization, the formation of just a few voids had a large effect on reducing coating adherence.

Nongraded $ZrO_2 \cdot Y_2O_3$ Coatings

The thermal cycling results and microstructural observations clearly indicated that the inclusion of a graded metal-to-zirconia layer detracted from coating adherence. Samples 3, 5, and 8 had either a very narrow or no graded transition layer. These samples performed well in the thermal cycling test.

No differences were observed in the performance of the two zirconia compositions: $ZrO_2 \cdot 20Y_2O_3$ (Samples 3 and 5) and $ZrO_2 \cdot 8Y_2O_3$ (Sample 8). Neither ceramic was affected by annealing at 1080°C; both retained the columnar microstructure and cubic crystal structure that was introduced during deposition. The $ZrO_2 \cdot 8Y_2O_3$ composition was of interest because it fell within the mixed cubic/tetragonal phase field. This ceramic composition was known to develop a two-phase microstructure with enhanced crack toughness (Porter and Heuer 1979; Green, Maki, and Nicholson 1974; Garvie and Nicholson 1972; Heuer 1981). However, in this study, x-ray diffraction patterns provided no evidence of tetragonal (or monoclinic) phase formation during the 1080°C annealing treatment, indicating that higher annealing temperatures would be needed before the desired two-phase microstructure would develop.

Examination of Samples 3, 5, and 8 in cross section following the thermal cycling experiment revealed that a very thin film of alumina had formed at the metal/ceramic interface. Some longitudinal cracking was also observed in the ceramic layer, usually near the base of the ceramic deposit. Both of these features represent a source of concern with respect to the long-term durability of the coatings.

The cracking of the ceramic was of greatest immediate concern. Sample 3 was much less prone to cracking than either of the other coatings. In fact,

after the fifth water quench, this sample was examined in the SEM and no spallation or surface cracks were observed. Some cracks were observed in the polished cross sections of the sample that were vacuum heat-treated at 1080°C for 8 h. However, these cracks ran vertically into the coating and usually stopped at the top of the graded zone; none were observed to penetrate into the CoCrAlY layer. In contrast, metallography on Samples 5 and 8 following heat treatment at 1080°C for 8 h showed that these samples developed longitudinal cracks in the pure ceramic layer parallel to the deposit surface. This cracking was in addition to the vertical cracking found in all the samples.

Two factors appeared to be important in reducing the amount of cracking in the ceramic layer. First, it was extremely important to obtain a stoichiometric deposit. In later experiments, O_2 was added to the sputtering gas during the deposition of the pure ceramic layer in Samples 3 and 6 through 9. These samples cracked much less in thermal cycling experiments than similar ceramic layers in Samples 4 and 5, where no supplemental oxygen was added.

The second factor that reduced cracking was the topography of the substrate. Sample 8 was the only deposit that covered an irregular surface. All of the longitudinal cracks observed in Sample 8 were in sections of the coating that covered a protuberance in the CoCrAlY layer. The ceramic layer was generally sheared off at the level of the surrounding ceramic outer surface; the cracking tended to produce a smooth outer surface by lopping off the high areas. It appeared that deposition of a flat ceramic coating on a smooth substrate surface improved the stress distribution within the ceramic layer and minimized the cracking of that layer.

MCrAlY-Al_2O_3 Coatings with Graded Transition Layers

Samples 10 and 11 were prepared with a graded MCrAlY-Al_2O_3 transition layer separating the metallic bond layer and the outer ceramic layer. These graded layers were expected to be thermodynamically stable, unlike the mixed MCrAlY-ZrO_2·Y_2O_3 deposits where free aluminum resulted in partial reduction of the zirconium oxide. Two ceramic layers were sputtered over graded alumina deposits: Al_2O_3·$40Cr_2O_3$ on Sample 10 and ZrO_2·$20Y_3O_3$ on Sample 11.

Upon heating, the graded region in both samples developed a fine dispersion of Al_2O_3 and metallic phases (Figure 17). This favorable microstructure appeared to be quite stable, as expected. Unfortunately, neither of the pure outer ceramic coatings adhered to the graded Al_2O_3 layer. Sample 11 spalled along the interface between the top of the graded CoCrAlY-Al_2O_3 layer and the outer $ZrO_2 \cdot Y_2O_3$ deposit as the sample was cooled at the end of the deposition experiment. The reason for this lack of adherence was not determined. However, ZrO_2 and Al_2O_3 are immiscible oxides and would not be expected to form a strong chemical bond.

On Sample 10, the $Al_2O_3 \cdot Cr_2O_3$ ceramic layer completely spalled upon initial heating. The failure of this layer was believed to be caused by stresses produced during crystallization of the amorphous, as-deposited phase; a phase transformation would have been accompanied by a 10% volume decrease. Separation occurred at the top of the graded zone, approximately where there was a 50:50 ratio (by weight) of metal to ceramic. This behavior suggests that grading to high alumina composition is detrimental and produces a metal/ceramic

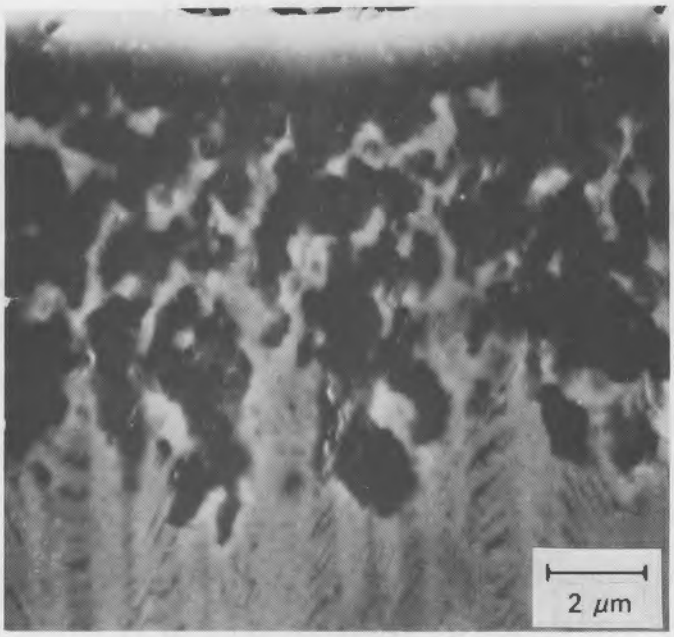

FIGURE 17. Microstructure Produced in Graded MCrAlY-Al_2O_3 Layer of Sample 12 After 8-h Heat Treatment at 1080°C

mixture that is weaker than pure ceramic. However, partial grading with alumina (to perhaps 40%) prior to ceramic deposition might improve ceramic adherence.

Mixed Metal/Ceramic Coatings

All of the coatings where deposition was terminated at the top of the graded zone (Samples 12 through 15) performed poorly in the thermal cycling experiment. Multiple cracking and spalling of the coatings were observed on all four of these samples. In particular, the Al_2O_3 coatings on Samples 12 and 14 were severely cracked, which was attributed to the phase transformation of the sputtered amorphous Al_2O_3 to α-Al_2O_3 upon heating.

Ceramic Closeout Layers

A second concern of the ceramic coatings task was the development of sealing layers for the segmented ceramic deposits. In complementary burner rig tests performed at Westinghouse (Andersson et al. 1982), it was demonstrated that the application of a dense closeout layer greatly extended the lifetime of porous ceramic coatings exposed to dirty fuel environments. These 500-h thermal cycling tests were conducted with No. 2 distillate fuels doped with either sea salt (100-ppm Na) or metal impurities (50-ppm V; 150-ppm Mg) to simulate sea-salt-contaminated fuels and residual fuels, respectively. Gas temperatures were maintained at 1200°C and metal temperatures ranged from 800 to 900°C.

A series of NASA plasma-sprayed $ZrO_2 \cdot 8Y_2O_3$ coatings were provided with dense, sputter-deposited overcoats of Pt, AlPt, and $ZrO_2 \cdot 20Y_2O_3$ by PNL (Andersson et al. 1982). The overcoats generally spalled during the test, although they extended the lifetime of the base coat by a factor of 1.5 to 2.7. Two thicknesses of overcoats were prepared: 5 μm and 18 μm. The coatings with the thicker closeout layers generally lasted 50% longer before cracking than the coatings covered with thinner closeout layers.

The lack of long-term adherence of the sputtered layers to the plasma-sprayed coatings was attributed at least in part to the irregular surface finish of plasma-sprayed coatings. Even when these coatings were polished prior to sputter deposition, the surface was quite irregular (Figure 18). The

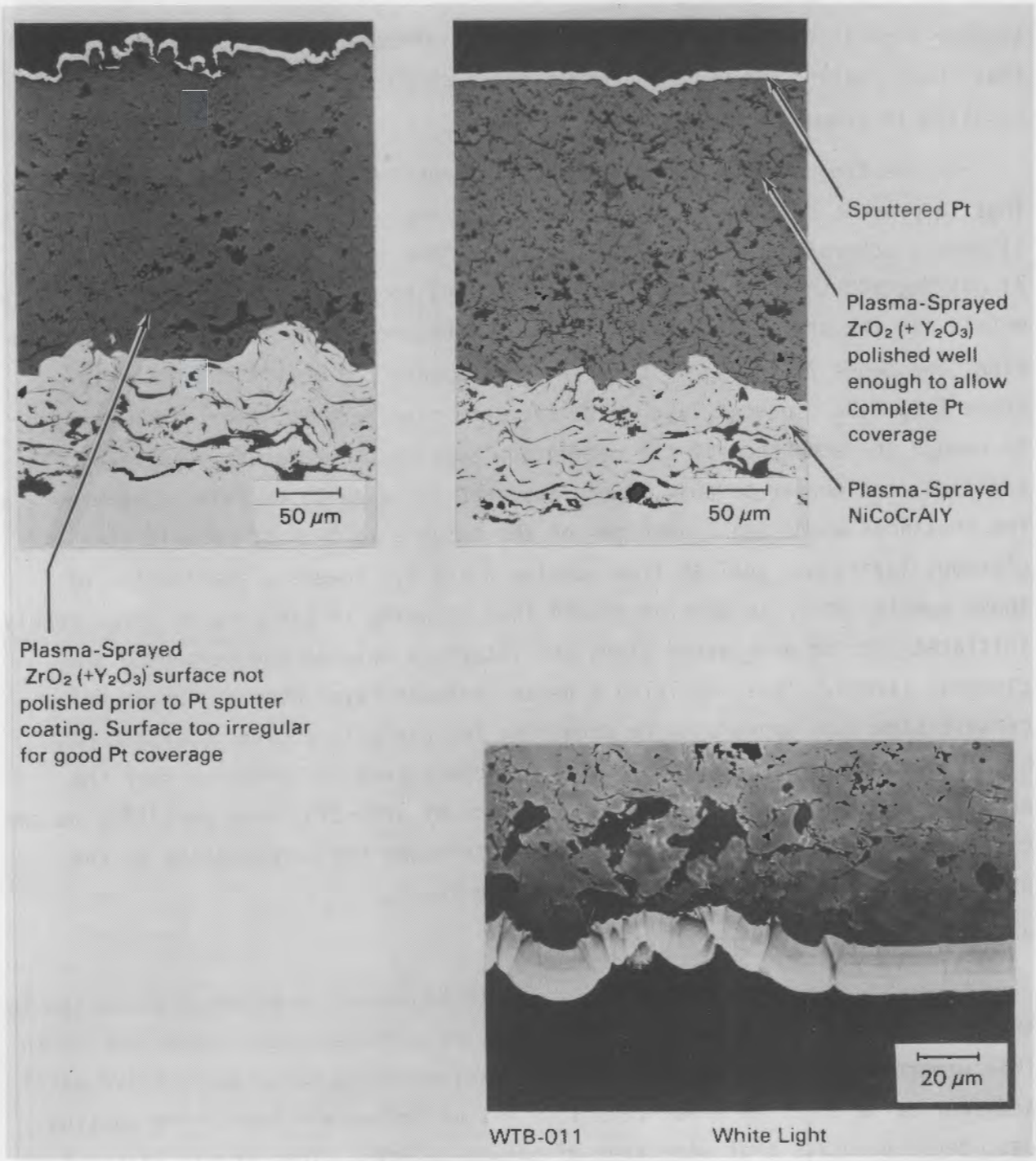

FIGURE 18. Examples of Sputtered Closeout Layers Deposited onto Plasma-Sprayed Coatings. Note the irregularity of the surface, even of coatings deposited on polished plasma-sprayed layers.

sputter-deposited overcoats replicated this surface roughness. It is believed that these coatings were nonuniformly stressed during heating and that this resulted in premature spallation.

The Westinghouse test demonstrated the necessity of sealing porous coatings to prevent contaminant infiltration. A successful closeout layer must: 1) remain adherent and relatively crack free for the life of the coating and 2) not degrade the adherence of the underlying porous ceramic layer to the base metal. In the short thermal cycling experiments described in the previous section, the dense $ZrO_2 \cdot Y_2O_3$ closeout layers appeared to meet these criteria. A dense $ZrO_2 \cdot Y_2O_3$ closeout layer over the segmented ceramic layer did not appear to reduce the adherence of the segmented layer to the metallic substrate. In addition, the denser ceramic layers appeared to be quite durable. There were a few instances where small sections of the outer 2 to 3 μm of ceramic (the closeout layer) had spalled from Samples 3 and 8. However, examination of these samples in cross section showed that cracking in the ceramic layer rarely initiated near or propagated along the interface between the segmented and closeout layers. Thus, applying a dense closeout layer over a segmented ceramic structure appears to be promising for use with engines operated on highly contaminated fuels. This dual structure provides porosity near the metal/ceramic interface to improve adherence by affording some ductility to the ceramic while the dense sealant overcoat minimizes the permeability of the overall coating to liquid and gaseous contaminants.

Multilayered Metal/Ceramic Coatings

The multilayered metal/ceramic deposits represent an alternative design to the coatings with a single ceramic layer. The multilayered coatings tested in this program (Figure 19) consisted of nine alternating thin layers (five metal and four ceramic ~25-μm thick layers). All of the metal layers were continuous, dense deposits that were free of growth defects. The ceramic layers contained a high density of growth defects (columnar voids) extending through each layer.

One of these coatings was mechanically tested to examine its fracture behavior. The sample was first notched from two sides and then pulled in tension to failure. The coating "sandwich" failed by a combination of ductile

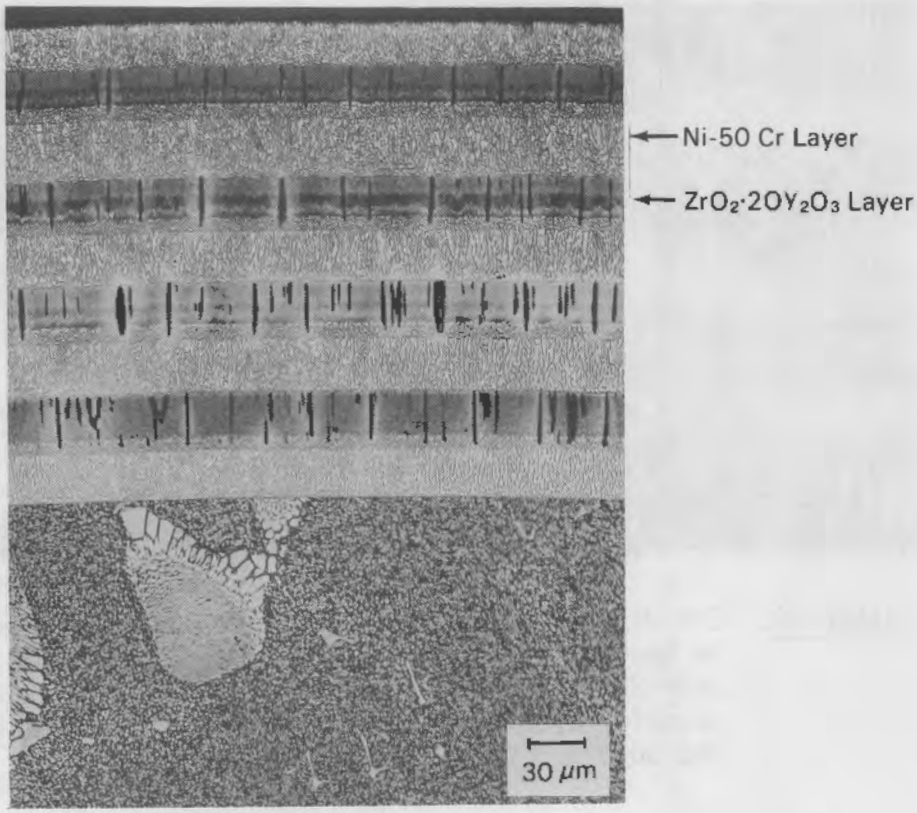

FIGURE 19. Optical Micrograph of Sputtered Nine-Layer Metal/Ceramic Coating

fracture in the Ni-Cr layers and brittle fracture (along columnar boundaries) in the ZrO_2. Extensive plastic deformation occurred in each of the Ni-Cr layers, with columnar grains rotating about 45° to accommodate shear between adjacent ZrO_2 layers. Prior to failure, the coating had sheared along the first ZrO_2 layer and the second Ni-Cr layer. Although some ZrO_2 columnar grains remained attached to the Ni-Cr layer (Figure 20), it was clear that this interface was the weakest part of the laminate structure.

As a preliminary test of the resistance of these coatings to thermal cycling, another pin was cycled 12 times in air between room temperature and 1100°C using a radiant furnace. Each cycle consisted of ~80 s of heating and ~120 s of cooling. No cracking, delamination, or other evidence of mechanical degradation was observed.

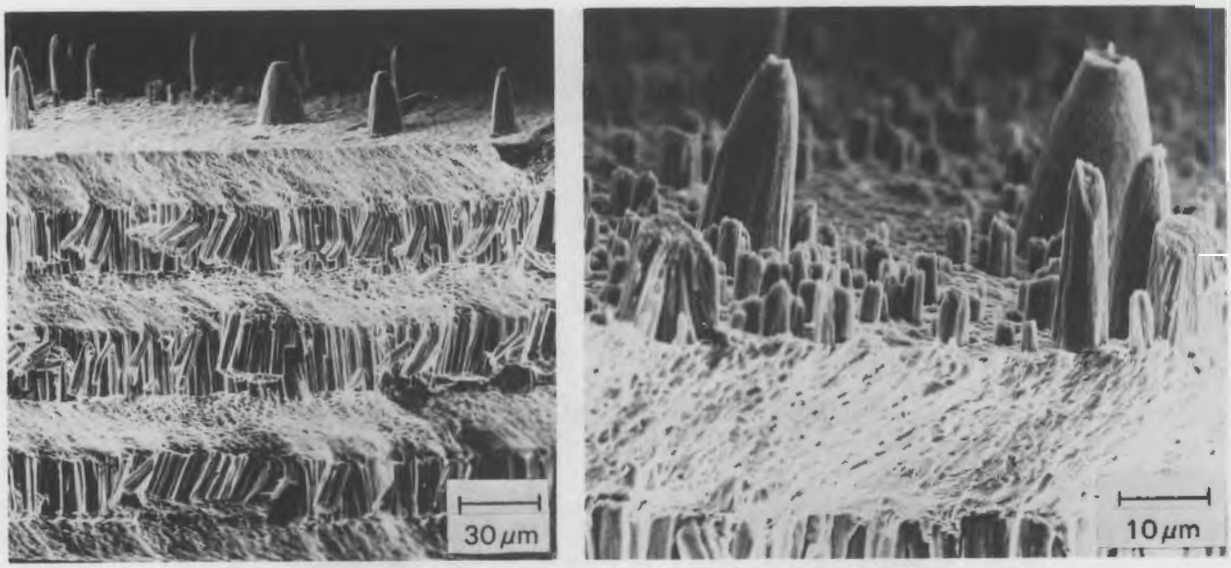

FIGURE 20. SEM Micrographs of Tensile-Tested Coating Showing Ductile Shear in Ni-50Cr Layers and Fracture Along Columnar Boundaries in the $ZrO_2 \cdot 20Y_2O_3$ Layers. Debonding occurred at the top of the lowest ceramic layer. The outer surface of the coating is located at the bottom of the micrograph on the left.

Finally, four multilayered coatings deposited on button samples were tested at Westinghouse. These 60-h thermal cycling tests (one thermal cycle per hour) were performed in a burner rig operated on either Na-doped fuel or V-doped fuel (Andersson et al. 1982). Gas temperatures were maintained at 1200°C. Three out of the four multilayered coatings failed by a combination of creep in the metallic layers and fracture of the innermost ceramic layer. Separation occurred between the first ceramic layer and the second NiCrAlY layer, similar to the results of the tensile test. The outer coating remained intact but was completely separated from the substrate; the substrate rattled freely inside the outer shell of coating. In addition, the metallic layers were highly oxidized. These results suggest that these coatings would have only limited use, perhaps in lower temperature applications (for example, erosive, low-temperature diesel applications).

SUMMARY

The tolerance of a series of oxide coatings to thermal cycling was studied. Zirconia coatings deposited directly onto metal bond layers had the best tolerance to thermal cycling. In general, a graded region between the metal bond layer and the outer ceramic coating detracted from the adherence of the ceramic layer. In the graded zirconia coatings, failures resulted from the massive redistribution of elements that occurred in the graded layer during annealing. Graded alumina layers were not affected by interdiffusion but still failed to improve ceramic adherence.

It appears that a dense closeout layer can be deposited over a columnar ceramic structure and not interfere with the ability of the segmented region to accommodate the lateral strains generated near the metal/ceramic interface. Use of this combination of porous and dense ceramic structures should permit development of adherent ceramic coatings with greatly reduced permeabilities to liquid and gaseous species. Such a coating would be well suited to the combustion atmosphere of highly contaminated alternative fuels such as coal-derived fuels or residual fuels.

Multilayered coatings consisting of alternate layers of metal and ceramic were judged to be of limited value. These coatings contained a large number of inherently troublesome metal/ceramic interfaces. In addition, the metal layers were very susceptible to oxidation.

SiC-METAL COMPOSITE COATING DEVELOPMENT

Replacing the current supply of highly refined petroleum-based fuels with alternatives such as residual fuels, coal-derived fuels, and coal-water slurries is expected to increase the severity of erosive/wear and corrosive conditions that engine components will experience. In particular, a severe wear problem can be anticipated as the concentration of abrasive contaminants increases in the fuel. Initial research is being directed at diesel engines where the earliest fuel substitutions are expected to occur. A major area of concern is with the wear surface between the top ring and the cylinder liner. At this point, temperatures are at their maximum and a condition of marginal lubrication can exist.

The objective of this task was to develop wear-resistant coatings for use in diesels operated on coal slurry fuels. The present generation of coal slurries consists of a close-packed array of 70-μm (75%) coal particles with smaller 30-μm (25%) particles filling the interstitial positions; all particles are suspended in either a water or oil media. Coatings used with these fuels will have to resist a severe combination of abrasive wear and particle erosion. High material hardness and good fracture toughness will be required to resist the resultant cutting and fatigue wear processes. This task sought to derive these properties from a plasma-sprayed coating with many ultrahard silicon carbide inclusions embedded in a ductile matrix. The inclusions provide hard points of contact, and the metal or glass matrix cushions the carbides against fracture from high-velocity particle impacts. If possible, a continuous hard surface layer was sought through a combination of hard inclusions and coal particles trapped in pockets that formed in the coating surface. Such a coating would offer good erosion resistance to engine components operating on coal slurry fuels.

Because of the premature termination of the CZD Program, testing with coal slurries was never completed. However, some preliminary experiments provided encouraging results. Promising coating compositions and techniques are discussed in this section.

EXPERIMENTAL PROCEDURES AND RESULTS

A series of composite coatings were prepared by plasma spraying. Preliminary experiments established deposition techniques that would be appropriate for further study. Samples were wear tested at 225°C using a ring-on-block apparatus and corrosion tested for 200 h in air at 600°C.

Coating Preparation

A SG-100 plasma spray system from Plasmadyne was used to prepare the composite coatings. The equipment operated at 40-kW power using both subsonic and Mach I plasma velocities. Two roto-feed hoppers with tapper assemblies were available for mixing two powders during the spray operation. However, the powders were usually premixed and fed from a single hopper because it was simpler and in most cases provided either comparable or superior powder feeding behavior. All coatings were deposited onto H-30 steel wear blocks that had been grit blasted prior to deposition.

Two forms of silicon carbide were tested: a fine powder and short fibers. The powder was 10 to 20 μm in diameter and was obtained from Cerac. Short fibers, 15-μm diameter x 0.5-cm, were cut from yarn obtained from Nippon Carbon Co., Ltd. Despite a number of attempts, no effective method of feeding the fibers to the spray gun was devised using Plasmadyne equipment. The fibers tangled, eventually leaving a congealed mass of fibers in the hopper that blocked the feed mechanism. Dilution of the fibers by premixing them with the matrix powder helped; but at the concentrations of interest (greater than 20 wt%), the fibers still tended to levitate to the top and then tangle. It was concluded that the only feasible solution would require adaptations to the gun to permit cutting and immediate feeding of the fibers to the gun, similar to those used in fiberglass production. Such modifications were not completed in this study.

Silicon carbide powders posed no handling difficulty. A series of ~250-μm thick coatings were prepared by spraying mixtures of silicon carbide and matrix material powders, either 410 stainless steel (SS) or SiO_2 (quartz). Two sizes

of 410 SS powder were used: a coarse-grained 44- to 74-μm powder and a fine-grained powder that was less than 44 μm in diameter. An ~50-μm diameter quartz powder was also used.

The SiC-quartz deposits were of interest since the quartz represented an inert and ductile (self-healing) matrix material. However, in preparing these coatings, it was found that thick deposits could not be prepared. As deposition proceeded, a very smooth surface formed that prevented subsequent buildup. Thus, these coatings were only 20 to 50 μm thick.

The 410 SS was chosen as a matrix material because of its good high-temperature fracture toughness and corrosion resistance. However, the combination of SiC and stainless steel proved disappointing. Combinations with greater than 12% SiC resulted in decreased wear resistance, apparently because of an increase in brittleness. It was felt that this could be due to the lack of a ductile matrix between SiC particles at higher carbide concentrations.

In later experiments, SiC particles were precoated with Ni using an electroless deposition technique (Krieg 1959) to minimize carbide-carbide contact. Approximately 50 g of SiC powder was first dipped in palladium chloride and then rinsed in water. The powders were transferred to a 1.5-liter bath of $NiSO_4 \cdot 6H_2O$ (39 g), $Na_2PO_2 \cdot H_2O$ (48 g), and lactic acid (30 g). This bath was adjusted to a pH of 5.0 and a starting temperature of 50°C. Once the powders were added, the batch was stirred continuously and heated to 95°C where Ni deposition accelerated. Two coatings were plasma sprayed using these Ni-coated SiC powders. One coating was made using a 50:50 mix of the coated carbide and the 410 SS; a second coating was prepared using only the precoated SiC powder.

Wear Test

Tribilogy samples were deposited onto flat H-30 steel blocks and then lapped prior to testing in a Falex-1 ring-on-block friction and wear tester. The coated wear block remained fixed and a rotating ring of hardened S-10 steel contacted the sample surface, generating a linear wear scar. The 3.5-cm ring rotated at 72 rpm and was loaded with 150 lb. A load cell measured the frictional force between the ring and the block. During the test, the samples were

immersed in an oil bath held at 225°C. The oil was Brayco 8999, an ACFT turbine engine lubricating oil. The test was terminated after 5000 ring rotations.

The wear test provided two pieces of data: 1) a wear scar width that indicated the extent of wear that had occurred during the test and 2) a final coefficient of friction that represented the status of the wear surfaces at the conclusion of the test. Figure 21 illustrates the dependence of the wear scar width on coating composition. These data provided a measure of the wear resistance of the coatings; a narrow wear scar indicated that little coating was abraded. Coefficient of friction data are presented in Table 9.

The majority of the coatings tested were 410 SS-SiC composite coatings. For these, there was a gradual decrease in wear scar width as small concentrations of SiC were added to the stainless steel coating. However, as the

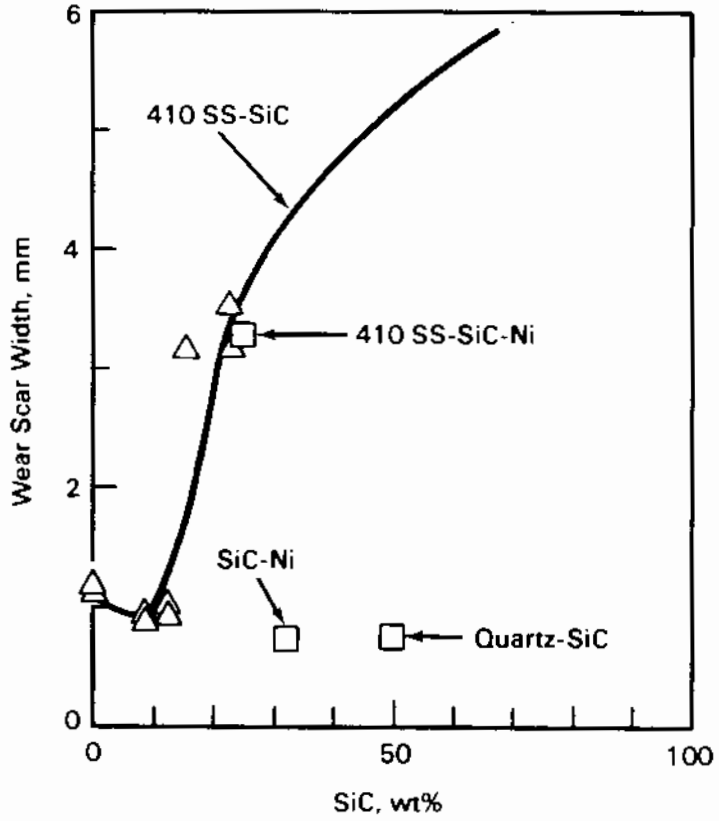

FIGURE 21. Wear Scar Widths for Different SiC Concentrations and Various Matrix Materials. Narrow wear scars indicate lower wear rates.

TABLE 9. Coefficient of Friction Data for SiC Composite Coatings

Sample	Description	Hardness	Coefficient of Friction
55	Fine 410 SS powder	315	0.143
56	Coarse 410 SS powder	233	0.141
50	Fine 410 SS + 8% SiC	321	0.144
51	Coarse 410 SS + 8% SiC	246	0.141
52	Fine 410 SS + 12% SiC	336	0.131
53	Coarse 410 SS + 12% SiC	217	0.137
57	Coarse 410 SS + 15% SiC	222	0.135
58	Fine 410 SS + 23% SiC	330	0.133
59	Coarse 410 SS + 23% SiC	253	0.137
60	Fine 410 SS + 70% SiC		0.132
61	Fine 410 SS + 50% SiC (Ni coated) (410 SS + 25% SiC + 25% Ni)	442	0.108
62	Ni-coated SiC (33% SiC)		0.090
54	Quartz + 50% SiC		0.110
48	Laystall: iron + 10% SiC	356	0.099
49	WC + 13% Co	1482	0.107

composition rose above ~12 wt% SiC, the width of the scar increased dramatically (rapid wear occurred). Changes in the particle size of the 410 SS powder used in spraying did not affect the wear behavior of the coatings. The use of SiC powder precoated with Ni and then mixed with 410 SS for spraying also failed to improve coating performance. For that mixture, the Ni coating on the SiC particles had been quite thin (~5 μm). In a later experiment, the SiC powder was processed through the Ni bath twice to provide a 10- to 15-μm Ni coating on the carbide particles. When this powder was sprayed alone, a Ni-30% SiC composite coating was deposited that had very good wear resistance. In addition, the quartz-SiC coating also demonstrated good wear resistance despite its limited thickness.

For comparison, a Laystall SiC-embedded iron sample with 10% SiC and a plasma-sprayed WC-13% Co powder coating were also tested. The first specimen was prepared by Laystall using a proprietary technique that impregnated an

ordinary iron cylinder liner with SiC and then honed the surface smooth. This technique improves the wear resistance of cylinder liners placed in diesels run on fuels cut with kerosene (Scott 1976). The kerosene is added to permit low-temperature operation; however, it also dissolves the lubricating oil and produces a severe wear problem. Impregnated linings and rings had performed well in this application. In the current test the Laystall coatings formed a wear scar of 1.13 mm, about the same as the 410 SS coatings. In addition, a WC-Co coating was prepared at PNL with powders obtained from Plasmadyne. This coating was very hard (1482 DPH) compared with other coatings (from about 215 to about 450 DHP). No well-defined wear scar was present on the coating surface. A significant weight loss occurred on the ring, suggesting that the wear occurred there rather than on the coatings.

The coefficient of friction data also provided a relative ranking of the coatings. All the 410 SS-SiC coatings had a coefficient of 0.14, while the others (the Ni-coated SiC, quartz-SiC, the Laystall, and the WC-Co coatings) had values around 0.10. The lowest coefficient of friction measurement was recorded on the Ni-SiC coating where a value of 0.090 was obtained. This result was encouraging since it suggested that a low wear rate condition may have existed by the end of the experiment and that long-term wear rates could be kept low.

Oxidation Test

These coatings were intended to be used in diesel engines under potentially severe erosive/corrosive conditions. Therefore, preliminary testing was performed to determine the oxidation resistance of the coatings. During preparation of the wear samples, duplicate coatings were plasma sprayed onto 18-mm diameter x 50-mm long steel rods. These samples were then oxidized at 600°C for 200 h in air. The WC-Co coating spalled badly during the test, eliminating it as a potential wear-resistant coating for use at elevated temperatures. All of the other coatings appeared to be in good condition after 200 h. No metallography was performed on the samples; therefore, the extent of oxidation was not determined. However, both the Ni-SiC and the quartz-SiC coatings were sufficiently oxidation resistant to justify further study.

SUMMARY

Two plasma-sprayed coatings were identified for potential use in diesels operated on alternative fuels. The first was a Ni-SiC composite that was sprayed using SiC powders precoated with nickel using an electroless deposition technique. The other was a quartz-SiC composite coating prepared by cospraying the two respective powders. The latter coating had a thickness limitation of about 50 μm. Both coatings displayed good wear and corrosion resistance and warrant further investigation.

CONCLUSIONS

As heat engines begin to operate on degraded fuel supplies, the problem of low-temperature hot corrosion will worsen. Current state-of-the-art CoCrAlY coatings can be modified to improve their low-temperature, hot corrosion resistance. Using chromium and aluminum composition gradients through the thickness of the coating and alloying CoCrAlY coatings with platinum were identified as useful coating modifications, although the exact modifications must be correlated with the application. The use of platinum underlayers as a diffusion barrier to limit substrate/coating interdiffusion was found to be ineffective.

In an aggressive, low-temperature, hot corrosion environment (simulated by burning doped marine diesel in burner rig), coatings with 1) a high chromium surface concentration, 2) a high chromium-to-aluminum ratio at the surface, and 3) an aluminum composition gradient that increased the aluminum concentration into the coating thickness were more corrosion resistant. Deposits of CoCrAlY containing large additions of platinum also provided good low-temperature protection.

A burner rig test with SRC-II provided materials data in an extremely aggressive environment (characteristic of vanadate attack). Of the coatings tested, those with 1) a low chromium surface concentration, 2) a high aluminum-to-chromium ratio at the surface, and 3) a chromium composition gradient that increased the chromium concentration into the coating thickness were more corrosion resistant.

In studies on zirconia- and alumina-based ceramic coatings, a graded transition layer between the metallic bond layer and the ceramic deposit did not improve ceramic adherence. Graded zirconia coatings failed as a result of massive diffusion of aluminum (from the MCrAlY bond layer) and oxygen (from the ZrO_2) in the graded metal-to-ceramic layer. Coating fracture occurred very low in the graded transition zone, where a band of Al_2O_3 and voids formed that acted as a preferred path for crack propagation. For this reason, the ZrO_2 coating with no graded transition zone performed the best in thermal cycling experiments. Graded Al_2O_3-CoCrAlY layers were not affected by interdiffusion; however, ceramic layers of $Al_2O_3 \cdot 40Cr_2O_3$ or $ZrO_2 \cdot 20Y_2O_3$ deposited over graded

Al_2O_3-CoCrAlY layers adhered poorly. Multilayered metal/ceramic coatings were judged to have only limited potential, perhaps in erosive low-temperature diesel applications.

Depositing dense closeout layers over the porous ceramic structure--for example, the columnar microstructure of PVD coatings--was identified as a potential technique for reducing the permeability of the coating to solid and liquid combustion products without affecting coating adherence. This or a similar sealing technique will be essential for the success of ceramic coatings used in alternative fuel environments.

In wear tests on silicon carbide composite coatings, plasma-sprayed coatings that deposited silicon carbide in either a nickel or quartz matrix had good wear and corrosion resistance. These coatings might be appropriate for use in diesels operated on erosive coal slurries.

REFERENCES

Andersson, C. A., et al. 1982. Advanced Ceramic Coating Development for Industrial/Utility Gas Turbine Applications. NASA CR-165619.

Aprigliano, L. F. 1980. Burner Test Results of Department of Energy/Battelle Northwest Coatings. U.S. Naval Ship Research and Development Center Report 10310, Annapolis, Maryland.

Barkalow, R. H., and F. S. Pettit. 1979. "Mechanism of Hot Corrosion Attack of Ceramic Coating Materials. In Proceedings of First Conference on Advanced Materials for Alternative Fuel Capable Directly Fired Heat Engines, NTIS Report CONF-790749, U.S. Department of Energy, Washington, D.C., pp. 704-714.

Bayne, M. A., et al. 1979. "Improvement of Sputtered Oxide Coating Adherence and Integrity for Turbine Airfoil Applications." In Proceedings of the First Conference on Advanced Materials for Alternative Fuel Capable Directly Fired Heat Engines, NTIS Report CONF-790749, U.S. Department of Energy, Washington, D.C.

Bratton, R. J., S. K. Lau, and S. Y. Lee. 1980. "Evaluation of Present-Day Thermal Barrier Coatings for Industrial/Utility Applications." Thin Solid Films 73:429-437.

Dapkunas, S. J., and R. L. Clarke. 1974. Evaluation of Hot-Corrosion Behavior of Thermal Barrier Coatings. U.S. Naval Ship Research and Development Center Report NSRDC-4428, Annapolis, Maryland.

Fairbanks, J., et al. 1975. "High-Rate Sputter Deposition of Protective Coatings on Marine Gas Turbine Hot-Section Superalloys." In Proceedings of 1974 Gas Turbine Materials in the Marine Environment Conference, NTIS Report MCIC-75-27, pp. 429-456.

Garvie, R. C., and P. S. Nicholson. 1972. J. Am. Ceramic Soc. 55(3):152.

Goebel, J. A., F. S. Pettit, and G. W. Goward. 1973. "Mechanism for the Hot Corrosion of Nickel-Base Alloys." Met. Trans. 4:261-278.

Goward, G. W. 1978. Thin Solid Films 53(2):223-224.

Green, D. J., D. R. Maki, and P. S. Nicholson. 1974. J. Am. Ceramic Soc. 57(3):136.

Grossklaus, W., N. E. Ulion, and H. A. Beale. 1977. "Some Effects of Structure and Composition on the Properties of Electron Beam Vapor Deposited Coatings for Gas Turbine Superalloys." Thin Solid Films 40:281-290.

Heuer, A. H. 1981. "Science and Technology of Zirconia." In Advances in Ceramics. Vol. 3, A. H. Heuer and L. W. Hobbs, eds., American Ceramics Society.

Hodge, P. E., R. A. Miller, and M. A. Gedwill. 1980. "Evaluation of the Hot Corrosion Behavior of Thermal Barrier Coatings." Thin Solid Films 73:447-453.

Krieg, A. 1959. "Processing Procedures." Presented at Symposium on Electroless Nickel Plating, ASTM Special Technical Publication No. 262, p. 21.

McKee, D. W., and A. P. Siemers. 1980. "Resistance of Thermal Barrier Ceramic Coating to Hot Salt Corrosion." Thin Solid Films 73:439-445.

McKee, D. W., et al. 1979. "Resistance of Thermal Barriers to Hot Salt Corrosion." In Proceedings of First Conference on Advanced Materials for Alternative Fuel Capable Directly Fired Heat Engines, NTIS Report CONF-790749, U.S. Department of Energy, Washington, D.C., pp. 258-269.

Nicholls, J. R., and P. Hancock. 1981. Burner Rig Testing of Advanced Coatings with SRC II Coal Derived Fuel. Final Report, Cranfield Institute of Technology, Bedford, England.

Patten, J. W. 1979. "The Influence of Surface Topography and Angle of Adatom Incidence on Growth Structure in Sputtered Cr." Thin Solid Films 63:21-129.

Patten, J. W., et al. 1977. In Proceedings of the 1977 Tokyo Joint Gas Turbine Congress, Gas Turbine Society of Japan, pp. 527-537.

Patten, J. W., et al. 1979a. "Development of Graded Composition CoCrAlY (+Pt) Sputtered Coatings." In Proceedings of First Conference on Advanced Materials for Alternative Fuel Capable Directly Fired Heat Engines, NTIS Report CONF-790749, U.S. Department of Energy, Washington, D.C., pp. 459-472.

Patten, J. W., et al. 1979b. "Sputter-Deposited Multilayered Ceramic/Metal Coatings." Thin Solid Films 64:337-343.

Patten, J. W., et al. 1980. "Mechanical Behavior of Segmented Oxide Protective Coatings." Thin Solid Films 73:463-470.

Patten, J. W., R. W. Moss, and D. D. Hays. 1980. Sputter Deposited Ceramic and Metallic Coatings Executive Summary. PNL-3609, Pacific Northwest Laboratory, Richland, Washington.

Porter, D. L., and A. H. Heuer. 1979. J. Am. Ceramic Soc. 62(5):298.

Ruckle, D. L. 1980. "Plasma Sprayed Ceramic Barrier Coatings for Turbine Vane Platforms." Thin Solid Films 73:455-461.

Scott, D. 1976. "Carbide Impregnation Cuts Cylinder Bore Wear." Automotive Engineering, December 1976.

Shen, S., D. Lee, and D. Boone. 1978. Thin Solid Films p. 233.

Stringer, J. 1976. "Hot Corrosion of High Temperature Alloys." In Properties of High Temperature Alloys, Z. A. Foroulis and F. S. Pettit, eds., ECS Proceedings, 77-1:513-556.

PNL-5013
UC-25

DISTRIBUTION

No. of Copies

OFFSITE

J. W. Byam, Jr.
U.S. DOE Morgantown Energy Technology Center
P.O. Box 880
Collins Ferry Road
Morgantown, WV 26505

L. Carpenter
U.S. DOE Morgantown Energy Technology Center
P.O. Box 880
Collins Ferry Road
Morgantown, WV 26505

J. W. Fairbanks
Office of Fossil Energy
Division of Advanced Energy Conversion
U.S. Department of Energy
MS FE-26
Germantown, MD 20767

27 DOE Technical Information Center

No of Copies

ONSITE

DOE Richland Operations Office

H. E. Ransom

70 Pacific Northwest Laboratory

E. L. Courtright (50)
S. K. Edler
C. R. Hann
D. D. Hays
R. W. Moss (5)
J. T. Prater (5)
Publishing Coordination (2)
Technical Information (5)